JGR Atmospheres

RESEARCH ARTICLE
10.1029/2018JD029791

Meteorological Conditions During an Ozone Episode in Dallas-Fort Worth, Texas, and Impact of Their Modeling Uncertainties on Air Quality Prediction

Xiao-Ming Hu[1,2], Ming Xue[1,2], Fanyou Kong[1,2], and Hongliang Zhang[3]

[1]Center for Analysis and Prediction of Storms, University of Oklahoma, Norman, Oklahoma, USA, [2]School of Meteorology, University of Oklahoma, Norman, Oklahoma, USA, [3]Department of Civil and Environmental Engineering, Louisiana State University, Baton Rouge, Louisiana, USA

Key Points:
- High ozone (O_3) concentration on a day with a "dead zone" in the Dallas-Fort Worth region is investigated with the dead zone being a key flow feature
- The benefit of ensemble is demonstrated for air quality forecasting
- The formation of the dead zone is linked to the atmospheric circulation pattern in the presence of Hurricane Irene in the western Atlantic displacing the Bermuda High

Supporting Information:
- Supporting Information S1

Correspondence to:
X.-M. Hu,
xhu@ou.edu

Citation:
Hu, X.-M., Xue, M., Kong, F., & Zhang, H. (2019). Meteorological conditions during an ozone episode in Dallas-Fort Worth, Texas, and impact of their modeling uncertainties on air quality prediction. *Journal of Geophysical Research: Atmospheres*, *124*, 1941–1961. https://doi.org/10.1029/2018JD029791

Received 9 OCT 2018
Accepted 14 JAN 2019
Accepted article online 16 JAN 2019
Published online 19 FEB 2019

Author Contributions:
Conceptualization: Xiao-Ming Hu, Hongliang Zhang
Data curation: Fanyou Kong
Funding acquisition: Ming Xue, Fanyou Kong
Methodology: Xiao-Ming Hu, Hongliang Zhang
Resources: Fanyou Kong
Visualization: Xiao-Ming Hu
Writing - original draft: Xiao-Ming Hu
Writing – review & editing: Xiao-Ming Hu, Ming Xue

Abstract The Southern Great Plains experiences an unhealthy level of ozone (O_3) at times. The formation mechanisms contributing to these O_3 events are not always clear and in some cases are related to particular atmospheric circulation patterns. A severe O_3 pollution event on 27 August 2011 in the Dallas-Fort Worth (DFW) area is investigated with a combination of observations and simulations using the Weather Research and Forecasting model with Chemistry (WRF/Chem). During the O_3 episode, a stationary front with a stagnant zone at the leading edge persisted to the west of DFW. At the time, Hurricane Irene was located in western Atlantic, displacing the Bermuda Subtropical High and affecting the circulations over the Southern Great Plains. The stagnant zone confined the pollutant plume originating from DFW, leading to accumulation of primary pollutants and prominent O_3 formation. Emission sources from a few urban areas east of DFW as well as power plants near Mount Pleasant and Carthage also contributed to this DFW O_3 pollution episode. This scenario is different from the typical summer days over the Southern Great Plains when southerly winds prevail along the west edge of the Bermuda High and the pollutant plumes from DFW are advected downstream, resulting in low O_3. Ensemble WRF/Chem predictions driven by the operational Short-Range Ensemble Forecast outputs are conducted to examine the impact of meteorological uncertainties (particularly transport uncertainties) on air quality forecasting. The ensemble mean gives a better prediction in terms of plume directions than individual members.

1. Introduction

Even though emission control regulations have been implemented for the past few decades, ozone (O_3) pollution in the lower troposphere remains an issue in the south central United States from time to time (Choi & Souri, 2015; Qin et al., 2007; Sather & Cavender, 2012). Summer O_3 episodes over the Southern Great Plains are often recorded (Hudak, 2014; Kim et al., 2009). Interestingly, O_3 episodes in the region have been observed to occur during the passage of Atlantic hurricanes (e.g., Hu, Zhang, et al., 2010; Nielsen-Gammon et al., 2010). The impact of hurricanes on air quality has been discussed in other regions (e.g., southeastern coast of China), and the impact reported had been limited to the vicinity of hurricanes (Huang et al., 2005; Jiang et al., 2015; Wang & Kwok, 2003; Wei et al., 2016; Yang et al., 2012); such studies do not address possible effects of hurricanes on a long distances such as Atlantic hurricanes on Southern Great Plains. The formation mechanisms of severe O_3 episodes, in particular the effects of meteorological factors associated with particular flow patterns, in the Southern Great Plains are not always clear.

According to the standard of daily maximum 8-hr average O_3 (70 ppbv), the Dallas-Fort Worth (DFW) metropolitan area in northern Texas is a nonattainment area (Digar et al., 2013; Pongprueksa, 2013), particularly in Collin, Dallas, Denton, Ellis, Johnson, Kaufman, Parker, Rockwall, Tarrant, and Wise counties (https://www3.epa.gov/airquality/greenbook/hbcs.html#TX). A few large field experiments, including the Texas Air Quality Studies in 2000 (referred to as TexAQS2000; Daum et al., 2004; Jiang & Fast, 2004; Wert et al., 2003) and in 2006 (referred to as TexAQS II; Parrish et al., 2009; Yu et al., 2012), have been conducted to investigate the sources and atmospheric processes responsible for the photochemical pollution during summer months in Texas, particularly the Houston and DFW metropolitan areas (Zhang

et al., 2013; Zhang & Ying, 2011). High O_3 episodes in DFW most often occur between May and October, especially during the months of August and September (Cox & Chu, 1996; Hudak, 2014). While elevated background O_3 concentrations were found to contribute to the O_3 exceedance in the DFW area (Kemball-Cook et al., 2009; Pierce et al., 2009), heavy pollution plumes originating from DFW were also demonstrated to be a cause using observational data (Langford et al., 2011; Luria et al., 2008; Senff et al., 2010) and model simulations (Kim et al., 2009; McKeen et al., 2009), suggesting significant contributions from local O_3 production.

In summer, westward extension of the Bermuda subtropical high favors the development of a southerly low-level jet over the Southern Great Plains, while transient processes (e.g., passages of frontal systems) may disturb such flow patterns at times (Klein et al., 2015; Lei et al., 2018; Zhu & Liang, 2013). During summer months, O_3 over the Southern Great Plains shows correlation with the Bermuda High variations: a stronger/weaker Bermuda High leads to lower/higher summer mean O_3 in the region with a magnitude of variation of around 6 ppbv (Zhu & Liang, 2013). During TexAQS II period in the summer of 2006, a strong pressure gradient along the west flank of the Bermuda High led to low O_3 over eastern Texas with 8-hr maximum O_3 ranging between 20 and 50 ppbv, while on high-ozone days with 8-hr maximum O_3 ranging between 60 and 65 ppbv, composite meteorology revealed a weak pressure gradient over eastern Texas associated with a high-pressure ridge (Wilczak et al., 2009). Many case studies also examined summer O_3 exceedances in the region, focusing mainly upon the Houston area (Banta et al., 2005; Daum et al., 2003; Karl et al., 2003; Kleinman et al., 2002, 2005; Rappengluck et al., 2008; Ryerson et al., 2003; Wert et al., 2003). While certain meteorological conditions (e.g., stagnant flows, high temperature) have generally been regarded as playing an important role in inducing O_3 pollution, the meteorological factors for the severe O_3 episodes in DFW remain uncertain (Kim et al., 2009; Luria et al., 2008). One of the purposes of this study is to demonstrate that synoptic-scale forcing and transport conditions play an important role in modulating ambient air quality in DFW during an episode associated with the Atlantic Hurricane Irene which made landfall in North Carolina in late August 2011.

Uncertainties in meteorological conditions, as well as errors in emissions, are the primary contributors to air quality forecasting uncertainties (Chatani & Sharma, 2018; Gilliam et al., 2015). Uncertainties in transport conditions represent a primary challenge in predicting urban air quality (Gilliam et al., 2015; Zhang et al., 2007). Such uncertainties need to be carefully considered in air quality evaluations and policy decision-making (Bei et al., 2016; Gilliam et al., 2012; Ludwig & Shelar, 1978; Pielke, 1998). While meteorological ensemble modeling has received much attention in both research and operational forecasting during the past three decades (e.g., Palmer et al., 1992; Stensrud et al., 1999; Toth & Kalnay, 1997), the use of ensembles of Eulerian dynamically generated meteorology-air quality models to characterize uncertainties of air quality forecast has been lagging behind (e.g., Bei et al., 2014; Delle Monache et al., 2006; Delle Monache & Stull, 2003; Djalalova et al., 2010; Galmarini et al., 2013; Marecal et al., 2015; McKeen et al., 2005; Monteiro et al., 2013; Vautard et al., 2009; Zhang et al., 2007). To achieve skillful probabilistic air quality forecasts, different approaches were used to construct the ensemble, including using multiple air quality models (Delle Monache & Stull, 2003; Djalalova et al., 2010; Galmarini et al., 2013; Marecal et al., 2015; McKeen et al., 2005; Monteiro et al., 2013; Vautard et al., 2009), perturbing emissions (Delle Monache et al., 2006), and perturbing meteorological conditions (Bei et al., 2014; Zhang et al., 2007). Perturbations to meteorological fields are shown to be critical for probabilistic air quality forecasts to capture temporal and spatial variation of pollutants such as O_3 (Delle Monache et al., 2006). The meteorological fields predicted by the National Weather Service operational Short-Range Ensemble Forecast (SREF) system (Du et al., 2009) were found by Gilliam et al. (2015) to be of good quality for examining the impact of meteorological uncertainties on retrospective off-line air quality simulations over the continental U.S. domain with a standalone chemical transport model (i.e., the Community Multiscale Air Quality (CMAQ) model). In this study, an ensemble air quality modeling system is set up by coupling SREF outputs and the Weather Research and Forecasting (WRF) model with Chemistry (WRF/Chem; Grell et al., 2005) to assess the uncertainties in urban air quality forecasting, particularly in forecasting urban plumes originating from DFW. Different from CMAQ, WRF/Chem is an online air quality model. The advantages and disadvantages of off-line and online air quality models are discussed in depth in Hu (2008). Also, different from the retrospective simulations of Gilliam et al. (2015), the SREF-WRF/Chem ensemble system is executed in a prediction mode without applying Four-Dimensional Data Assimilation (FDDA) that constrains the simulated

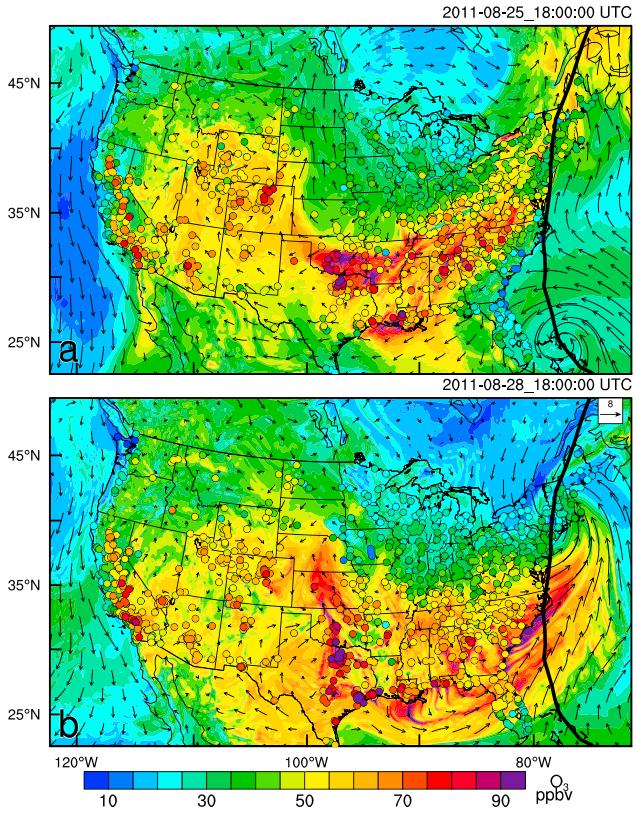

Figure 1. Simulated O_3 and wind fields in the first domain by the control WRF/Chem deterministic simulation on (a) 25 and (b) 28 August 2011 overlaid with observed O_3 concentration (shaded circles) at the U.S. Environmental Protection Agency (EPA) air quality system (AQS) sites. The official track of hurricane Irene on the eastern coast of United States is marked.

meteorological fields using observations, so as to examine the effect of meteorological forecast uncertainties on urban air quality prediction.

The rest of this paper is organized as follows. Section 2 describes the selected air pollution episode, observations, and design of deterministic WRF/Chem simulations and the SREF-WRF/Chem ensemble forecasting system. Section 3 examines the contributing factors for the air pollution event through the deterministic simulations and discusses impact of uncertainties of meteorological fields on air quality forecasting using SREF-WRF/Chem outputs. Section 4 reviews previously reported impacts of fronts on surface O_3 and further discusses the different role of the front revealed in this study on O_3 formation associated with Atlantic hurricanes. Conclusions are summarized in section 5.

2. Data and Methods

2.1. Episodes and Observational Data

On 25–29 August, Hurricane Irene moved from east of Cuba to northeastern United States. After making landfall at the North Carolina coast on 27 August, it moved more or less along the northeastern Atlantic coast of the United States and eventually became an extratropical cyclone on 29 August, by which point its center was located near the New Hampshire and Vermont border (Figure 1). Meanwhile, the DFW metropolitan area experienced the most severe O_3 pollution of the summer of 2011 (O_3 in August is shown in Figure 2a). On 27 August 2011, 19 out of 20 Texas Commission on Environmental Quality (TCEQ) air quality sites in the DFW metropolitan area recorded 8-hr O_3 averages of >75 ppbv (https://www.tceq.texas.gov/cgi-bin/compliance/monops/8hr_monthly.pl). The TCEQ sites are part of the U.S. Environmental Protection Agency Air Quality System (AQS). The Rockwall site on the east side of DFW (Figure 3), experiencing a daily maximum of 8-hr average O_3 of 73 ppbv, was the only site in the DFW metropolitan area with maximum 8-hr average O_3 lower than 75 ppbv on 27 August; this day had the greatest number of sites experiencing unhealthy levels of O_3 during August of 2011. Revealing the contributing meteorological factors for this severe O_3 pollution event is the first goal of this study.

For comparison, air quality was comparatively good during 6–8 August 2011. The maximum O_3 concentration on 8 August is near the monthly minimum (Figure 2a). During this period, the synoptic forcing is steady, with a strong west-to-east pressure gradient supporting southerly prevailing winds in Texas. This period was studied in Hu and Xue (2016) in terms of inland penetration of the sea breeze and its impact on the nocturnal urban heat island and secondary O_3 maximum in DFW.

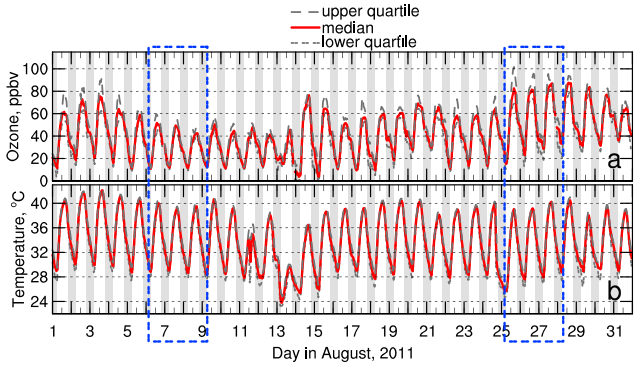

Figure 2. Time series of (a) O_3 and (b) temperature observed at the 20 TCEQ sites in the DFW metropolitan area (see their locations in Figure 3) in the month of August 2011. Two periods (i.e., 6–8 and 25–27 August) analyzed in this study are marked. Periods of sunset to sunrise are shaded.

The periods of 25–27 August (referred to as the high-ozone period hereafter) and 6–8 August 2011 (low-ozone period) are selected for detailed analyses in this study in terms of O_3 air quality and the contributing factors using both observational data and model simulations, with particular focus on 27 and 8 August. In addition to illustrating the temporal variation of air quality, the O_3 data at the 20 TCEQ sites around DFW (Figure 3) are used to examine the spatial distribution in the metropolitan area.

The regional meteorological conditions are examined using the Surface Weather Observations and Reports for Aviation Routine Weather Reports (METAR) data archived by the Meteorological Assimilation Data Ingest System (MADIS) of the National Oceanic and Atmospheric Administration (NOAA). High Vertical Resolution Radiosonde Data at

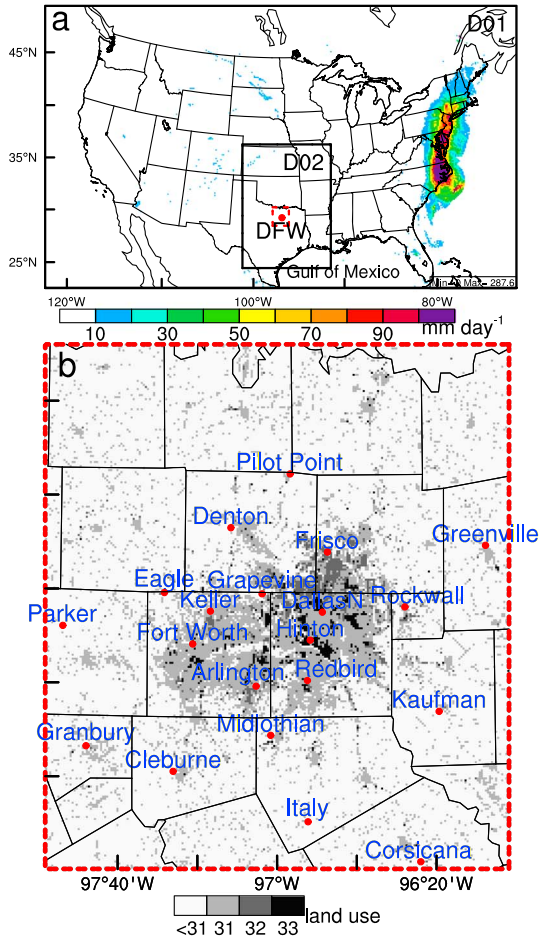

Figure 3. (a) Domain configuration of WRF/Chem simulations with stage IV average daily precipitation on 26 and 27 August 2011 showing in shaded color and (b) the 20 TCEQ air quality sites in the DFW metropolitan area with the three urban land use categories (i.e., 31, 32, and 33) shaded.

Fort Worth (32.83508°N, 97.29794°W) are used to examine the boundary layer structure; radiosonde data are only available at the standard observation times of 1200 UTC (0600 CST) and 0000 UTC (18 CST). The actual radiosonde launch times can be ~1 hr before the official observation time, while ascent of the sounding balloons can take up to an hour.

2.2. Three-Dimensional Deterministic Simulations

Deterministic WRF/Chem simulations are first conducted to diagnose factors contributing to the severe O_3 episode on 25–27 August 2011. One control simulation is conducted for each selected period (i.e., 6–8 and 25–27 August) with WRF/Chem version 3.7.1 (Grell et al., 2005). Here deterministic means that no perturbation is introduced into the model initial or boundary condition, as in ensemble forecasts described in next section. Two one-way nested domains (Figure 3a) are employed with horizontal grid spacings of 12 and 4 km, respectively. Each domain has 48 vertical layers extending from the surface to 100 hPa. The sigma levels and middle-layer heights of the lowest 20 model layers are shown in Table 1. Both grids use the Dudhia shortwave radiation algorithm (Dudhia, 1989), the rapid radiative transfer model (Mlawer et al., 1997) for longwave radiation, Yonsei University planetary boundary layer scheme (Hong et al., 2006), and the WRF Single-Moment six-class microphysics scheme (Hong et al., 2004). The Noah land surface scheme (Chen & Dudhia, 2001) coupled with a single-layer urban canopy model (Kusaka et al., 2001) is used to simulate land surface processes. Such a configuration was demonstrated to capture the thermodynamic and dynamic effects of urban areas in the Southern Great Plains quite well (Hu et al., 2017; Hu & Xue, 2016). The urban land use categories (Figure 3b) are derived from the National Land Cover Data 2011 (Homer et al., 2015), in which the urban land use is divided into three categories: low-intensity residential (31), high-intensity residential (32), and commercial/industrial (33).

Since the National Centers for Environmental Prediction operational Global Forecast System analysis was reported to have a cold bias resulting from excessive moisture in the southeast Texas (Hu, Nielsen-Gammon, et al., 2010; Hu, Zhang, et al., 2010; Kim et al., 2011), the 0.7° × 0.7° European Centre for Medium-Range Weather Forecasts ERA-Interim reanalysis is used for initial conditions (for both domains) and boundary conditions (for the outer domain) of meteorological variables. The boundary conditions of the inner domain are obtained from the outer domain simulation through one-way nesting. To obtain the best meteorological fields for air quality diagnosis (Kim et al., 2010), the FDDA analysis nudging procedure in WRF is applied. Temperature, water vapor, and wind variables are nudged toward the analysis fields available at 6-hourly intervals but linearly interpolated to the integration time steps.

The gas-phase chemical reactions are simulated using the Regional Atmospheric Chemistry Mechanism (Stockwell et al., 1997), which is implemented within WRF/Chem using the Kinetic Preprocessor (Sandu et al., 2003). Hourly anthropogenic emissions of chemical species come from the 4 km × 4 km national emission inventory for year 2011. Biogenic emissions are calculated using the Model of Emissions of Gas and Aerosols from Nature (MEGAN; Guenther et al., 2006). The simulations are initialized at 0000 UTC on 6 and 25 August and run for 84 hr. Our analysis will focus on 8 and 27 August 2011. The initial and boundary

Table 1
Sigma Levels and Midlayer Heights (m agl) of the Lowest 20 Model Layers

Sigma Levels	1.0	0.997	0.994	0.991	0.988	0.985	0.975	0.97	0.96	0.95
Middle-layer heights	12	37	61	86	111	144	186	227	290	374
Sigma levels	0.94	0.93	0.92	0.91	0.895	0.88	0.865	0.85	0.825	0.8
Middle-layer heights	459	545	631	717	826	958	1092	1226	1409	1640

Table 2
Details of the 12 SREF Members Used in the SREF-WRF/Chem Ensemble System[a]

Perturbations \ Models	ARW	Eta	NMM
n1	Member 1	Member 2	Member 3
n2	Member 4	Member 5	Member 6
P1	Member 7	Member 8	Member 9
p2	Member 10	Member 11	Member 12

[a]p1, p2, n1, and n2 represent the two positive and negative perturbations of each SREF model (Gilliam et al., 2015).

conditions for the chemical species are extracted from the output of the global model MOZART4 with a resolution of 2.8° × 2.8° (Emmons et al., 2010).

Sensitivity simulations are designed to isolate/identify the impact of Hurricane Irene on the meteorological conditions around DFW and the subsequent effects on the O_3 pollution episode on 27 August 2011. Approaches of (1) turning off latent heating from microphysics (referred to as no_mp_heating) (This option in WRF turns off microphysics latent heating in both model domains. Such simulations are often called "fake dry" simulations) and (2) lowering sea surface temperature (SST) over the Atlantic Ocean are adopted in sensitivity simulations to suppress the development of the hurricane. The amplification of moist convection is driven by the release of latent heat through condensation (Houze & Betts, 1981). Turning off latent heating in the microphysics scheme suppresses the development of moist convection (Hu, Fuentes, et al., 2010; Juneng et al., 2007; Taraphdar et al., 2014; Yamamoto, 2012; Zhang et al., 2003), thus suppressing hurricane development. During the 27 August O_3 episode, precipitation associated with Hurricane Irene dominated over the whole continental U.S. domain with daily mean precipitation on 26–27 August along the eastern coast exceeding 100 mm/day and single-point precipitation rate reaching ~300 mm/day (Figure 3a) while precipitation in central United States or on the nested 4-km grid is minimal. Thus, the dominant effect of turning off latent heating is mainly Hurricane Irene and related circulations. Lowering the SST reduces latent heat flux and sensible heat flux over the ocean, also suppressing hurricane development (Fitzpatrick, 1997; Tory & Dare, 2015). In the sensitivity simulations, FDDA analysis nudging is turned off to allow the hurricane to be suppressed through physics processes.

2.3. Ensemble Forecasting With the SREF-WRF/Chem Ensemble System

Ensemble forecasting is conducted with the SREF-WRF/Chem system to quantify the impact of meteorological uncertainties on air quality prediction on 27 August 2011. The SREF system was developed by the National Centers for Environmental Prediction of the U.S. National Weather Service for regional ensemble weather forecasting (Tracton et al., 1998) and the system has been operational at National Centers for Environmental Prediction since 2001 (Du & Tracton, 2001). In 2011, SREF consisted of 21 ensemble members using four weather prediction models: the Eta model (Black, 1994; Janjić, 1990), the Advanced Research WRF (ARW; Skamarock et al., 2008), the Nonhydrostatic Mesoscale Model (NMM) version of WRF, and the Regional Spectral Model (RSM; Juang & Kanamitsu, 1994). Each model was used for a certain number of ensemble members, and the members had different initial and boundary condition perturbations. The grid spacings of the SREF members were between 32 and 35 km. The SREF system was run 4 times each day starting from 03, 09, 15, and 21 UTC. A more detailed description of SREF can be found in Gilliam et al. (2015). Due to compatibility issues with WRF/Chem, only 12 SREF members are used in this study to drive WRF/Chem forecasting (i.e., using the SREF outputs to provide initial and boundary meteorological conditions). These 12 SREF members used the WRF-ARW, Eta, and WRF-NMM models with perturbed initial conditions (see Table 2). The SREF-WRF/Chem ensemble system is applied in a free forecast mode without FDDA nudging. The SREF forecast cycle initialized at 2100 UTC (15 CST) 26 August 2011 is used to initialize

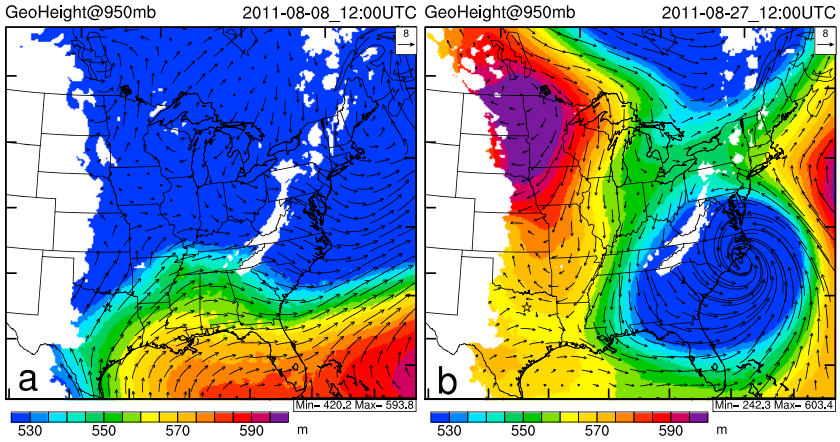

Figure 4. Simulated geopotential height and wind fields at 950 mb at 1200 UTC on (a) 8 August and (b) 27 August 2011. Dallas is marked with a star.

the WRF/Chem predictions into 27 August to allow enough time for solution spin-up on the high-resolution 4-km grid, while still keeping the forecast length short enough for better forecast accuracy.

3. Results

3.1. Synoptic Meteorological Forcing

The large-scale meteorological forcing for the two selected periods is first examined. During the 25–27 August high-ozone episode, a high-pressure center persisted at 500 hPa over west of the Southern Great Plains (including Oklahoma and Texas) and southwest United States (including New Mexico and Arizona). In the atmospheric boundary layer (e.g., at 900–950 hPa), a high-pressure center moved into the central Great Plains and a high-pressure ridge extended into northern Texas (Figure 4b). Consequently, a surface front formed in the Southern Great Plains and became stationary in the northeastern corner of Texas on 27 August 2011 (Figure 5b). A similar high-pressure ridge also showed up in eastern Texas on the high-ozone days during the second Texas Air Quality Study (TexAQS II) period in the summer of 2006 (Wilczak et al., 2009). In contrast, during the low-ozone period (i.e., 6–8 August), the high pressure at 950 hPa (part of the Bermuda High) extended west from the Atlantic Ocean to the Gulf of Mexico (Figure 4a), which supported the southerly or southwesterly boundary layer flows over Texas (Figures 4a and 6a). This pressure pattern is similar to the composite pressure field calculated by Wilczak et al. (2009) for low O_3 periods in eastern Texas. The surface wind observations archived in the MADIS data confirmed the above analyzed flow patterns for the two periods, with strong southerly winds in eastern Texas on 8

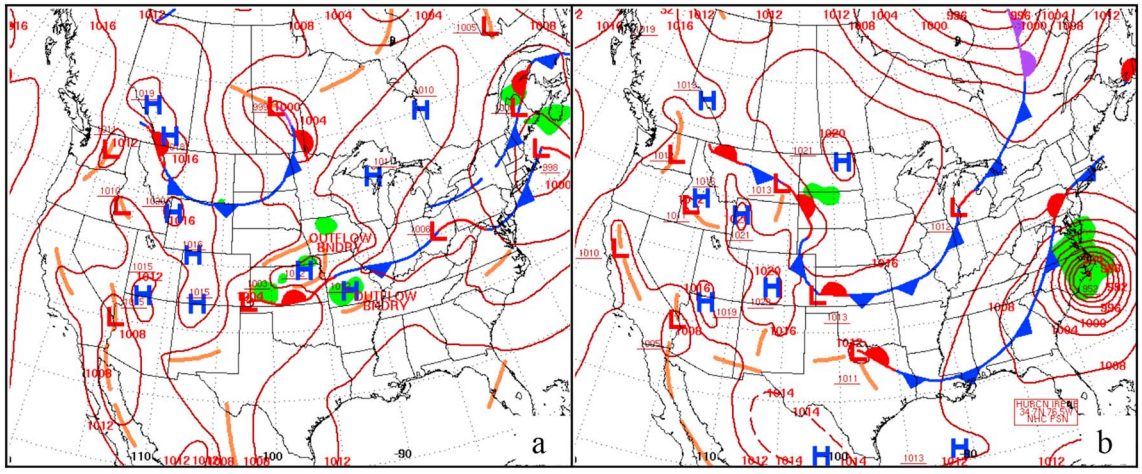

Figure 5. Weather maps at 1200 UTC on (a) 8 August and (b) 27 August 2011, which were prepared and archived by the Hydrometeorological Prediction Center of the National Centers for Environmental Prediction (http://www.wpc.ncep.noaa.gov/dailywxmap/).

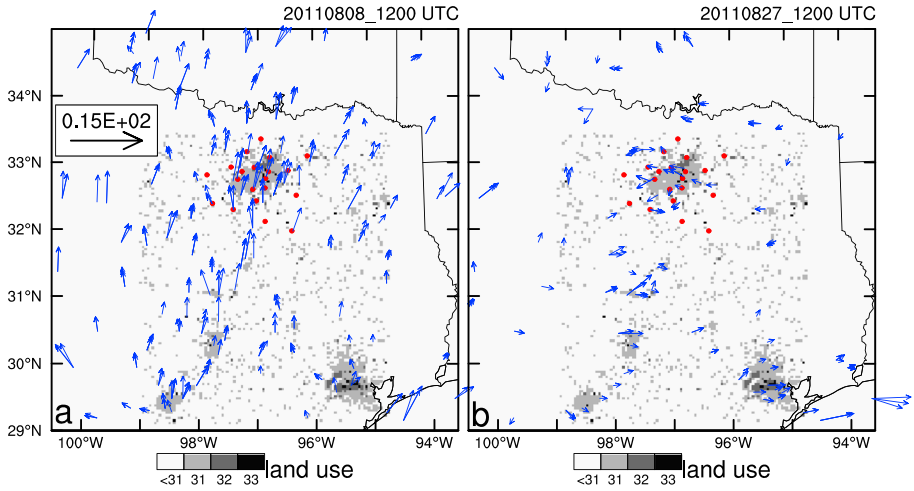

Figure 6. MADIS METAR observation at 1200 UTC on (a) 8 August and (b) 27 August 2011. The red dots indicate the locations of the TCEQ air quality sites in the DFW metropolitan area.

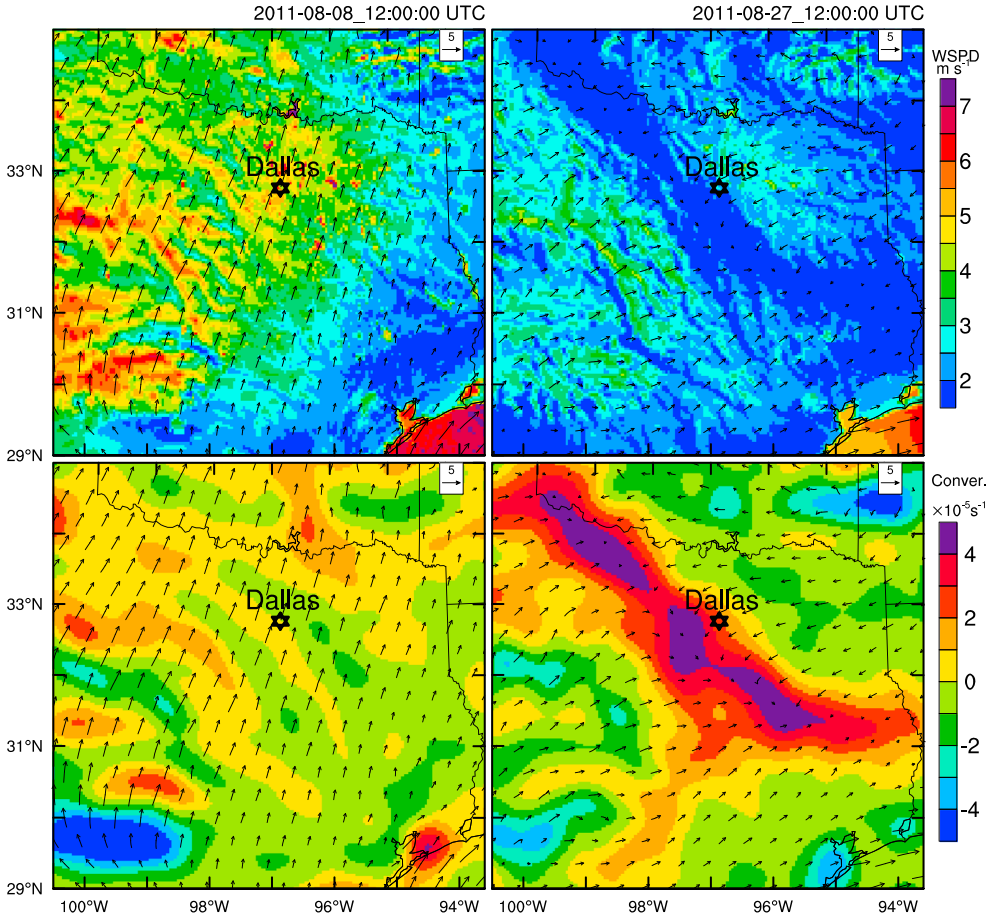

Figure 7. (top) Wind speed and (bottom) convergence simulated by the control simulations at 1200 UTC on (left) 8 August and (right) 27 August 2011. Simulated wind vectors are overlaid.

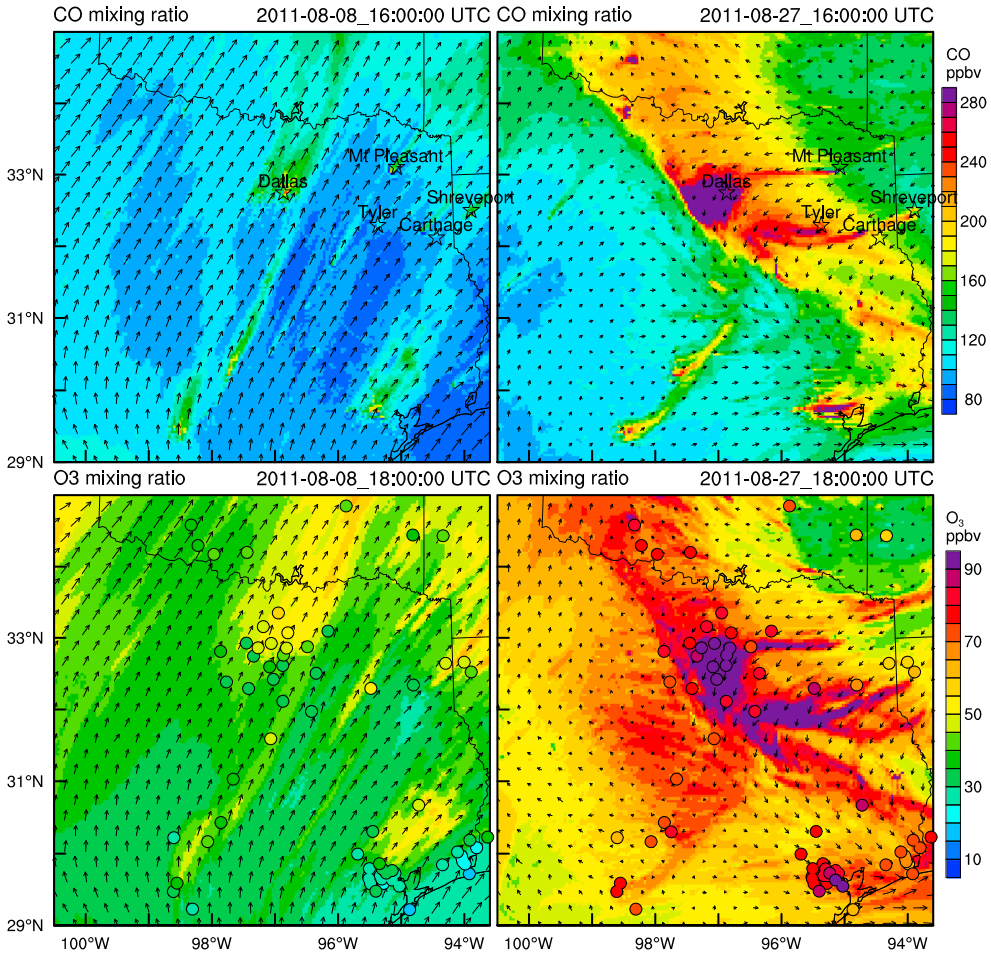

Figure 8. Spatial distribution of (top) CO and (bottom) O_3 plumes on (left) 8 August and (right) 27 August 2011 simulated by the control deterministic simulations. The observed O_3 values at the EPA AQS sites are indicated by shaded circles.

August (Figure 6a) and a confluence line associated with the stationary front west of DFW on 27 August 2011 (Figure 6b).

3.2. Diagnosing Factors Contributing to the Severe O_3 Episode Using Simulation Experiments

3.2.1. Analysis of the Control Simulations for the Selected Two Periods

The control WRF/Chem deterministic simulations capture the observed surface wind patterns on 8 and 27 August quite well. Uninterrupted southwesterly flow over Texas is simulated on 8 August (Figure 7), and a persistent northwest-southeast oriented confluence line is simulated around DFW on 27 August with wind direction transition from easterly (northeast of the confluence line) to southwesterly (southwest of the confluence line) across the line. Such deformational flows produce strong convergence and a stagnation zone with low wind speeds along the confluence line. The location of the confluence line (Figure 7) matches the location of the observed front (Figures 5b and 6b). These results indicate that the stationary front led to a deformation field, which induced a low wind speed zone west of DFW on 27 August. Such a low wind speed zone is referred to as the "dead zone" by McNider et al. (2005).

The confluence zone along the sea/lake/bay breeze head has been reported to play an important role in near-surface pollution events in many places around the world, such as Los Angeles (Angell et al., 1972), cities around the Lake Michigan (Lyons et al., 1995), Mid-Atlantic United States (Martins et al., 2012; Stauffer et al., 2015; Stauffer & Thompson, 2015), Houston (Banta et al., 2005; Bao et al., 2005; Darby, 2005; Zhang et al., 2007), and Beijing (Miao et al., 2015). To the best of our knowledge, however, identification of the dead zone associated with fronts and confirmation of its impact on air quality have not been discussed in prior literature.

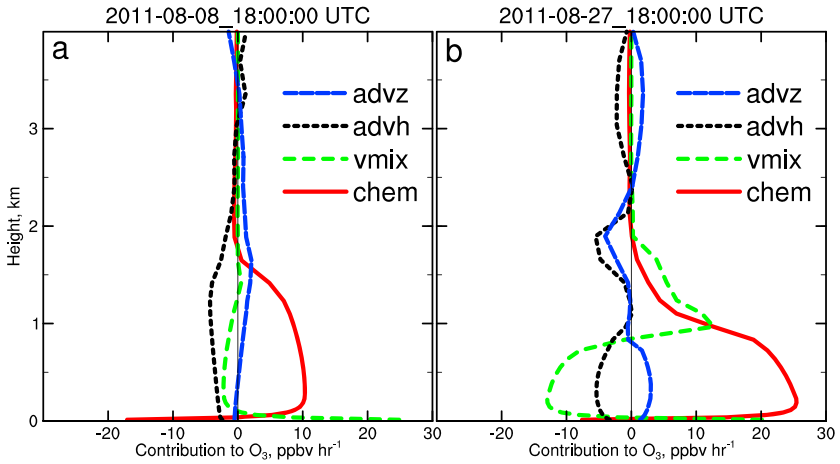

Figure 9. Contribution to O_3 accumulation over the DFW metropolitan area by different processes, including vertical advection (advz), horizontal advection (advh), vertical mixing (vmix), and chemical reactions (chem) at 1800 UTC on (a) 8 August and (b) 27 August 2011.

The impact of the confluence zone induced by the stationary front on air quality in DFW is illustrated in Figure 8. Model simulations successfully capture urban plumes originating from DFW, in terms of the spatial distributions of observed O_3 at TECQ sites for both episodes. On 8 August, when the southerly/southwesterly winds were not interrupted by mesoscale weather systems such as fronts, the plume of carbon monoxide (CO, a primary pollutant) from the DFW extended far downwind into Oklahoma. As a consequence, the O_3 plume (produced through photochemical reactions among the primary pollutants in presence of sunlight) also extended into Oklahoma (Figure 8). These results corroborate the conclusions of Klein et al. (2014) that interstate transport may have contributed to the air pollution in Oklahoma in certain circumstances. However, since the urban plume from DFW is stretched thin on 8 August 2011, the concentrations of the primary pollutants are low and O_3 formation is relatively low. Thus, the O_3 concentration in the DFW metropolitan area is relatively low on this day (Figure 8). The flow and air quality pattern of 8 August falls into the scenario of a low O_3 "breeze" over the Southern Great Plains that occurs when the Bermuda High prevails, as reported by Zhu and Liang (2013).

In contrast, with the northwest-southeast oriented stationary front persisting in the southwest of DFW on 27 August, the primary pollutants are confined and accumulated in the vicinity of DFW (as indicated by CO in Figure 8) in presence of northerly/northeasterly wind over DFW. As a result, afternoon O_3 formation in the pollutant plume from DFW is substantial, with boundary layer O_3 reaching ~110 ppbv (free troposphere O_3 is often around 50–60 ppbv). Sustained moderate northerly winds in the afternoon in DFW cause a short, southward O_3 plume, that is, high O_3 concentration in the southern part of the metropolitan area. The distinct O_3 plumes confirm that local O_3 production plays an important role in O_3 exceedances in DFW, which is consistent with the results of Kim et al. (2009), which suggest that O_3 production from local emissions may contribute as much as ~50 ppbv to daytime O_3 in DFW. Figure 8 also illustrates that winds dictate the dispersion direction and extent of primary pollutants, which further determine the subsequent O_3 formation and the spatial distribution of O_3 concentration in the DFW metropolitan area, corroborating the conclusion of Hudak (2014) that population and vehicle miles traveled play less important roles than wind in modulating the O_3 distribution in DFW.

In addition to the dominant pollution plumes in the DFW metropolitan area, there are a few easily discernable plumes east of DFW; surface CO concentrations indicate that these emission plumes originate from urban areas such as Mount Pleasant, Carthage, Tyler, and Shreveport. Kim et al. (2011) previously also reported dominant nitrogen oxide sources from the power plants near Mount Pleasant and Carthage. These emission sources lead to discernable O_3 plumes. At 1800 UTC (1200 CST), 27 August, the O_3 plume originating from Mount Pleasant already extends into the DFW metropolitan area, partially contributing to this DFW O_3 pollution episode.

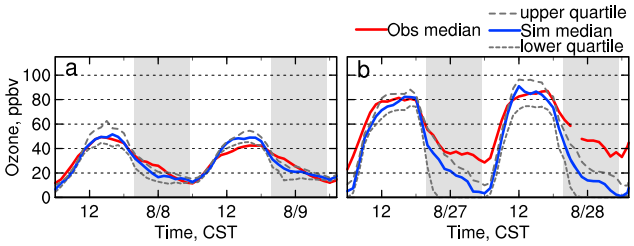

Figure 10. Observed and simulated O_3 concentration in the DFW metropolitan area during (a) 7–9 August and (b) 26–28 August 2011. Periods of sunset to sunrise are shaded.

Process analysis is conducted to further examine the contribution of various processes to the boundary layer O_3 accumulation in the DFW metropolitan area. For both episodes, during late morning through early afternoon, chemical production dominates, compared to other processes such as advection and vertical mixing, in the increase of the boundary layer O_3 (Figure 9). However, chemical production in the boundary layer on 27 August (~25 ppbv/hr) is more pronounced than on 8 August (~10 ppbv/hr), presumably due to different accumulation of primary pollutants as discussed above. Note that chemical reactions produce O_3 in the middle to upper boundary layer but decrease O_3 near the surface (Figure 9) because surface emission of nitric oxide (NO) acts to quickly remove O_3 near the surface through the titration process, while complex chemical reactions involving nitric oxides and volatile organic compounds start to produce O_3 at higher altitudes (Hu et al., 2012; Sillman, 1999). Once O_3 is produced in the middle of the boundary layer, vertical mixing processes disperse it upward through the upper boundary layer and downward to the surface. Thus, vertical mixing contributes positively to O_3 accumulation near the surface but negatively in the middle of the boundary layer (Figure 9).

Time series of O_3 in the DFW metropolitan area and vertical profiles observed by radiosondes at Fort Worth are also used for evaluation of the control WRF/Chem simulations. The model captures daytime O_3 and the difference between the high-O_3 and low-O_3 periods quite well (Figure 10), with a high correlation coefficient of 0.9 and a low bias of −2.1 ppbv (Table 3). However, the model underestimates the nighttime O_3 during the high-O_3 episode when the background wind is relatively weak. The mean bias of simulated nighttime O_3 is −13.3 ppbv (Table 3). The model simulates zero O_3 concentration at some sites while observations indicate certain levels of O_3. Urban O_3 on low wind nights is dictated by removal processes (i.e., NO titration and dry deposition) and downward transport (Klein et al., 2014; Kulkarni et al., 2015). The substantial low O_3 bias on the nights of 26–28 August indicates that surface O_3 is excessively depleted by the titration reaction and/or dry deposition while the downward transport of richer O_3 upper layer air is too weak on the relatively stable night in the model simulation. Overly weak downward transport of O_3 during stable nights is presumably due to underestimated vertical mixing for chemical species in WRF/Chem (Matichuk et al., 2017; Pleim et al., 2016). Due to the deficiency in the coupling between the meteorological and chemical components in WRF/Chem, nonlocal mixing and entrainment processes are neglected for chemical species (Hu et al., 2012; Hu, Klein, & Xue, 2013; Pleim, 2011), resulting in an underestimate of nighttime downward transport of richer O_3 in WRF/Chem, particularly on relatively stable nights.

Table 3
Statistics Evaluation for the Simulated O_3 at the 20 Air Quality Sites in the DFW Metropolitan Area During the Two Selected Periods[a]

Metrics	Overall	Day (7-18CST)	Night
Mean obs	44.416	54.527	34.653
Mean sim	36.603	52.425	21.329
Number of data	2956	1452	1504
corr	0.83	0.90	0.54
MB	−7.812	−2.102	−13.325
MAGE	11.888	8.331	15.322
RMSE	16.615	11.206	20.526
NMB	−17.6%	−3.9%	−38.5%

[a]The statistical metrics include correlation coefficient (corr), mean bias (MB), mean absolute gross error (MAGE), root-mean-square error (RMSE), and normalized mean bias (NMB). Formulas for these metrics can be found in Seigneur et al. (2000). These statistical metrics are commonly used in numerical model evaluations (e.g., Han et al., 2008; Hu, Klein, & Xue, 2013; Yu et al., 2006; Zhang et al., 2014). The statistics are calculated for all the hours, daytime only, and nighttime only.

The radiosondes at ~0000 UTC (1800 CST) at Fort Worth are used to evaluate the simulated convective boundary layer structures in late afternoon on 8 and 27 August 2011 (Figure 11). The boundary layer top can be identified from the profiles of both meteorological and chemical profiles. The boundary layer heights are ~2 to 2.5 km on 8 and 27 August. WRF/Chem successfully captures the observed boundary layer structures in terms of meteorological variables (with a slight underestimation of boundary layer height on 8 August). Simulated O_3 formation in the boundary layer on 27 August is prominent, while boundary layer O_3 formation on 8 August is weak and the boundary layer O_3 is even lower than that in the free troposphere. Unfortunately, no O_3 data are available in the soundings for evaluation of the simulated O_3 profiles.

3.2.2. Diagnosing the Role of Hurricane Irene Using Sensitivity Simulations

Given WRF/Chem's satisfactory performance during the two selected periods, the no_mp_heating sensitivity WRF/Chem simulation, which turns off latent heating from microphysics, was conducted for 25–27 August 2011 to investigate the impact of Hurricane Irene on meteorological conditions and the resulted O_3 formation over north central Texas. With

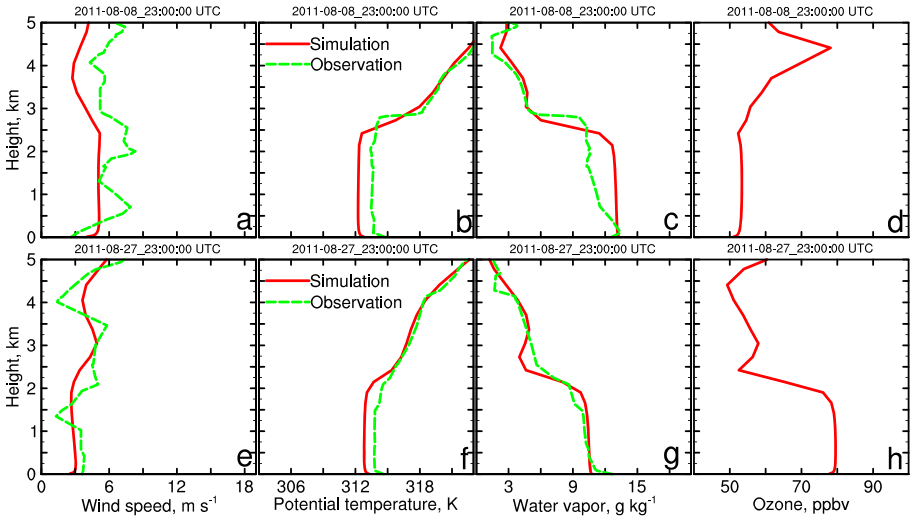

Figure 11. Vertical profiles of wind speed, potential temperature, water vapor mixing ratio, and O_3 at Fort Worth on (top) 8 August and (bottom) 27 August 2011.

condensation latent heating turned off, the hurricane is greatly suppressed in terms of size and intensity (Figures 12b and 12d). The lateral boundary conditions, however, are the same between the sensitivity and control simulation, and thus, the lateral boundary conditions may still provide forcing to produce a vortex in the domain. With a suppressed hurricane, a high-pressure area in the southeast part of the domain forms, which supports strong southwesterly flow over DFW, similar as the normal condition when the Bermuda High prevails. The strong southwesterly flow leads to a high dispersion over DFW and transports the emission plume far downward to Oklahoma (Figure 13b). As a result, O_3 production is

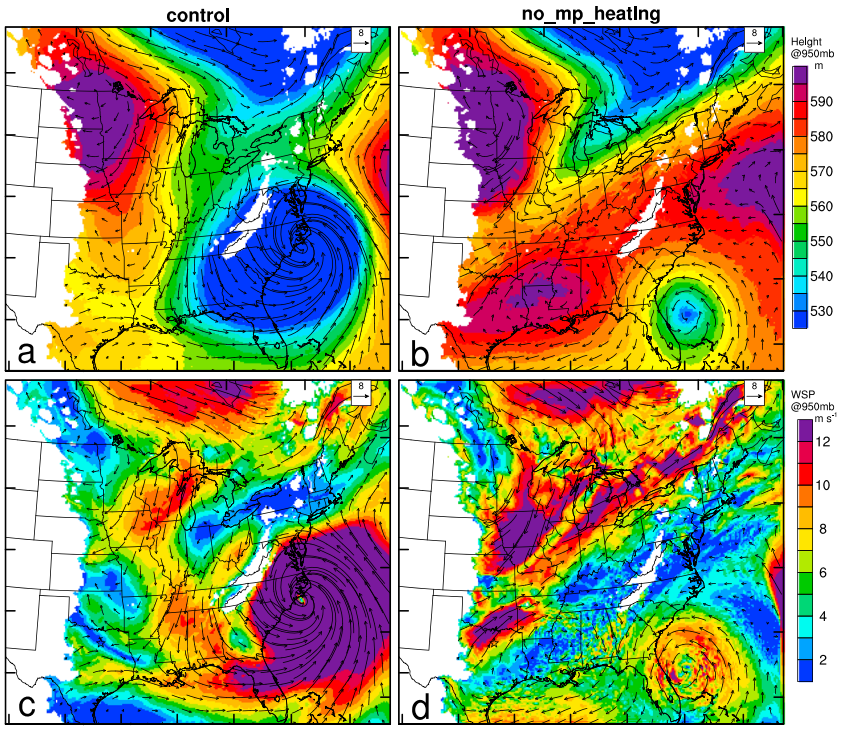

Figure 12. Simulated (top) geopotential height and (bottom) wind speed at 950 mb at 1200 UTC on 27 August 2011 by (left) the control and (right) no_mp_heating simulation. Simulated wind vectors are overlaid and Dallas is marked with a star on each panel.

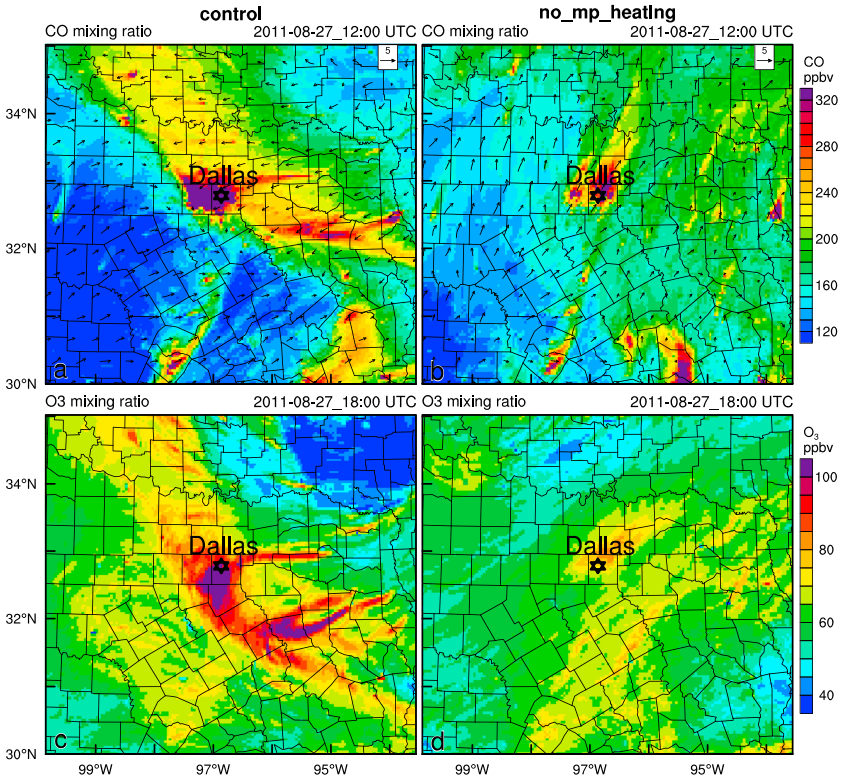

Figure 13. Spatial distribution of (top) CO and (bottom) O_3 plumes on 27 August 2011 simulated by (left) the control and (right) no_mp_heating simulations.

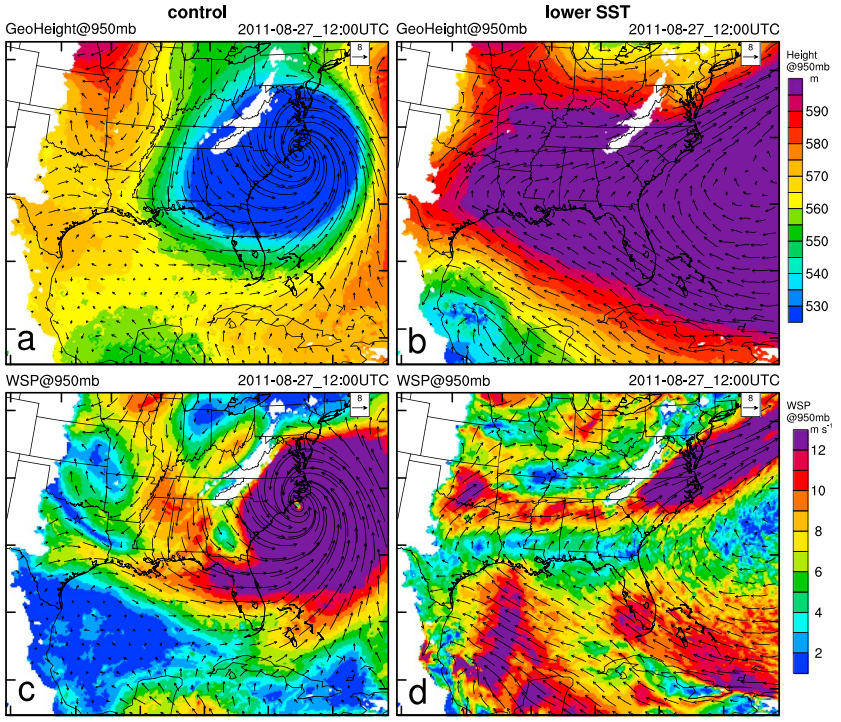

Figure 14. Simulated (top) geopotential height and (bottom) wind speed at 950 mb at 1200 UTC on 27 August 2011 by (left) the control and (right) "lower SST" simulation. Simulated wind vectors are overlaid and Dallas is marked with a star on each panel.

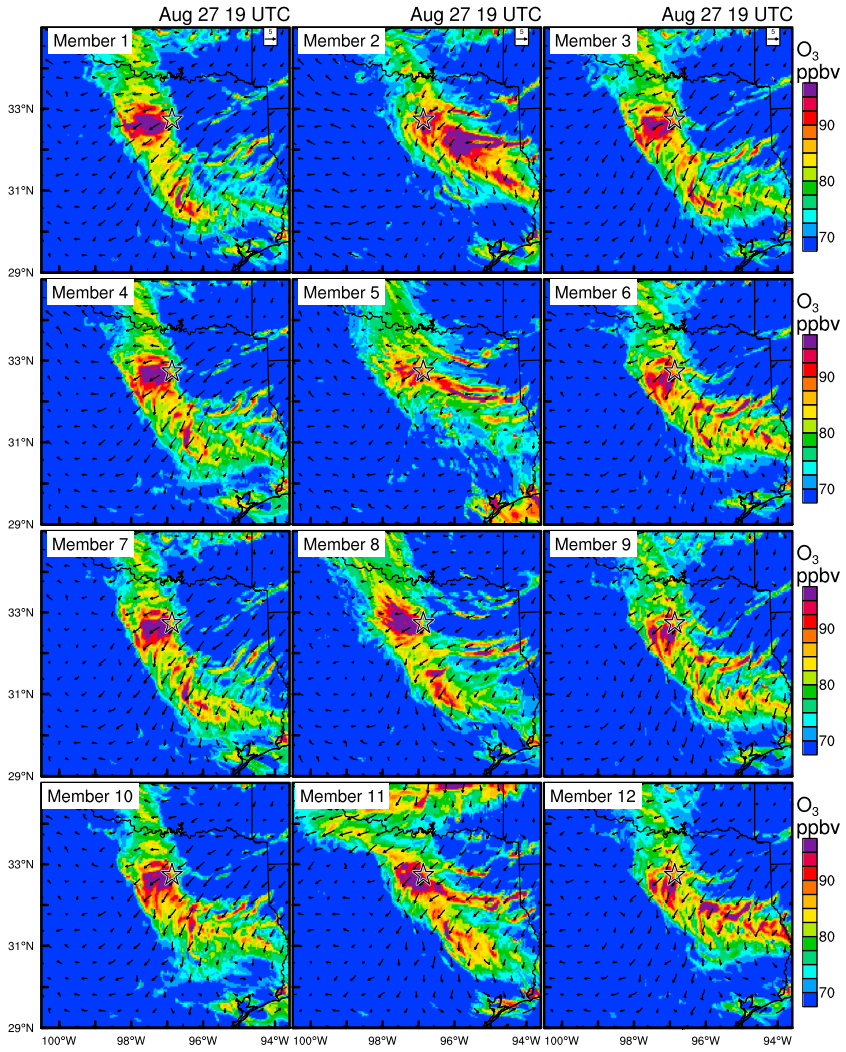

Figure 15. Ozone concentration and wind fields at 1900 UTC (1300 CST) on 27 August 2011 predicted by the SREF-WRF/Chem ensemble members. Dallas is marked with a star.

much weaker and the mixing ratio in the O_3 plume from DFW is only ~80 ppbv (Figure 13d), compared to ~110 ppbv in the control simulation (Figure 13c).

Another approach to isolate the impact of Irene is to suppress it through lowering SST over the Atlantic Ocean only. By lowering SST over the Atlantic Ocean by 8 K from 22 August when Irene is still in its early stage, the Hurricane Irene barely develops. Hurricane Irene is virtually gone on 27 August 2011 and Bermuda High extends westward into the Southern Great Plains as in the typical summer days (Figure 14). The southerly/southwesterly winds over Dallas on the west flank of the Bermuda High lead to good dispersion conditions as on normal summer days (Figure 14d). As a result, primary pollutants such as CO are dispersed as far as Oklahoma and O_3 formation over Dallas is weak (figure not shown). Note that we tested lowering SST over the Atlantic Ocean from 22 August by 5 K; a vortex still develops.

3.3. Examining the Impact of Meteorological Uncertainties on O_3 Prediction Using Ensemble Forecasts

Given the importance of meteorological fields (particularly transport) on modulating O_3 plumes as discussed above, errors in meteorological fields should play a very important role in inducing uncertainties to O_3 prediction. Quantifying the uncertainties of air quality prediction caused by uncertainties of meteorological fields is important for air quality evaluations and policy decision-making (Gilliam et al., 2012; Ludwig & Shelar, 1978; Pielke, 1998). Thus, the SREF-WRF/Chem ensemble system is run from the 2100 UTC 26

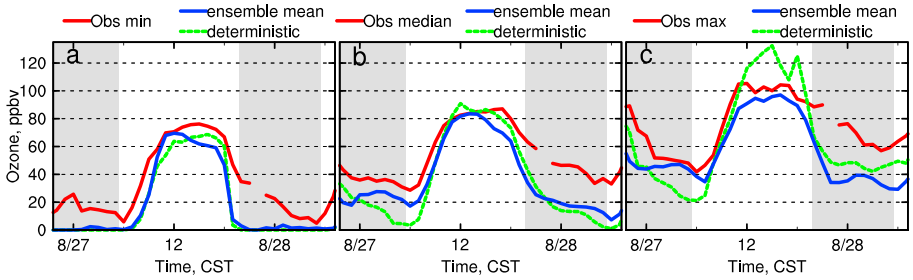

Figure 16. (a) Minimum, (b) median, and (c) maximum O_3 concentration at the 20 air quality sites in the DFW metropolitan area observed and predicted by the control deterministic simulation and SREF-WRF/Chem ensemble mean.

August SREF initial conditions for assessing O_3 prediction uncertainties on 27 August 2011. All members predict a northwest-southeast oriented region of low wind speed near DFW on this day, as in the control simulation discussed in the previous section and their distance from DFW is slightly different (figure not shown). At 1900 UTC (1300 CST) 27 August, most ensemble members predict a prominent O_3 plume from DFW except members 2 and 5 (Figure 15). In a few members (e.g., members 2, 5, and 11), there are prominent O_3 plumes from urban areas such as Shreveport, Mount Pleasant, and Tyler east of DFW, which extend into the DFW area. Thus, these urban emissions may contribute to O_3 pollution in the DFW area under certain meteorological conditions (e.g., easterly wind).

The capability of the ensemble mean to capture the maximum, minimum, and median O_3 among the 20 air quality sites around DFW is compared with the control deterministic simulation (Figure 16). Note that there are a few differences between the ensemble simulations and the control deterministic simulation. The 2100 UTC 26 August SREF initial conditions used by the ensembles did not have the benefit of 0000 UTC 27 August sounding and other observations, as in the deterministic simulations using European Centre for Medium-Range Weather Forecasts analysis as initial and nudging conditions; also, the ensemble forecasts are purely free forecasts without FDDA nudging while the control deterministic experiment of the previous section is run in a retrospective mode with FDDA nudging. Both the ensemble mean and control deterministic simulation perform similarly, capturing the minimum and median O_3 at the 20 sites. They accurately capture daytime median O_3 (Figure 16b), while slightly underestimating the daytime minimum O_3 (Figure 16a). During nighttime, both of them underestimate O_3, presumably due to the deficiency of the coupling between meteorological and chemical components in WRF/Chem mentioned earlier. The underestimation of nighttime O_3 increases with increasing forecast lead time into the second night. The ensemble mean and control deterministic simulation perform markedly differently for daytime maximum O_3 over DFW. The deterministic simulation significantly overestimates maximum O_3 (by >20 ppbv) while the ensemble mean slightly underestimates daytime maximum O_3 on 27 August (Figure 16c). Given the different plume directions from different members (Figure 15), the ensemble mean has the effect of smoothing out the local extreme O_3 values.

In contrast to the daytime statistical O_3 values (i.e., median, maximum, minimum) in the DFW metropolitan area, for which the SREF-WRF/Chem ensemble prediction system performs well with high consensus, the system gives a large spread in terms of O_3 plume direction. Certain individual members (e.g., member 2) have distinctly different DFW O_3 plumes from other individual members (Figure 15). The ensemble mean shows the capability to roughly capture the DFW O_3 plume (see the example at 1400 CST in Figure 17a). Even though the ensemble predicts the location of the extreme O_3 values (>100 ppbv) in the DFW metropolitan area slightly displaced (Figure 17b), the ensemble shows a better capability to capture the location of less extreme O_3 values (e.g., >90, >80 ppbv; Figures 17c and 17d). The ensemble captures most of the sites with O_3 values >80 ppbv with high percentage chances; that is, most members capture those O_3 values/locations, except the ensemble misses two sites over the northeast of DFW (Figure 17d). When the DFW O_3 plume moves southwest in this afternoon, the ensemble has ability to capture the leading edge of the plume, but the O_3 concentrations in the rear of the plume decrease too quickly. At the leading edge, O_3 experiences an increasing stage; while in the rear of the plume, O_3 experiences a decreasing stage in its diurnal cycle. This indicates that the model has a better capability to capture the increasing stage in the

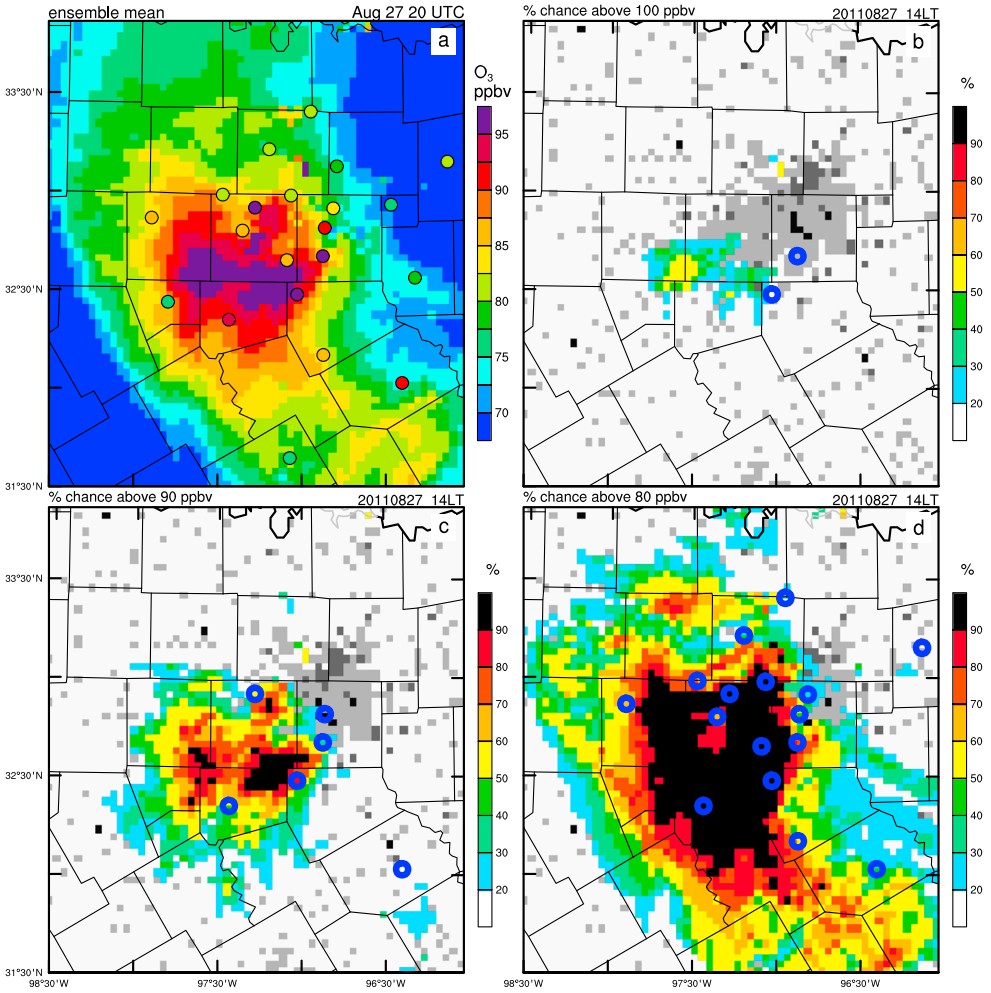

Figure 17. (a) Ensemble mean O_3 overlaid with observed O_3 mixing ratios (shaded circles) in the DFW metropolitan area, and percentage chance of the ensemble to simulate O_3 values over three threshold values, that is, (b) >100, (c) >90, and (d) >80 ppbv, with the observed O_3 over the individual threshold indicated by the blue circle. Urban land use is shaded in gray in (b–d).

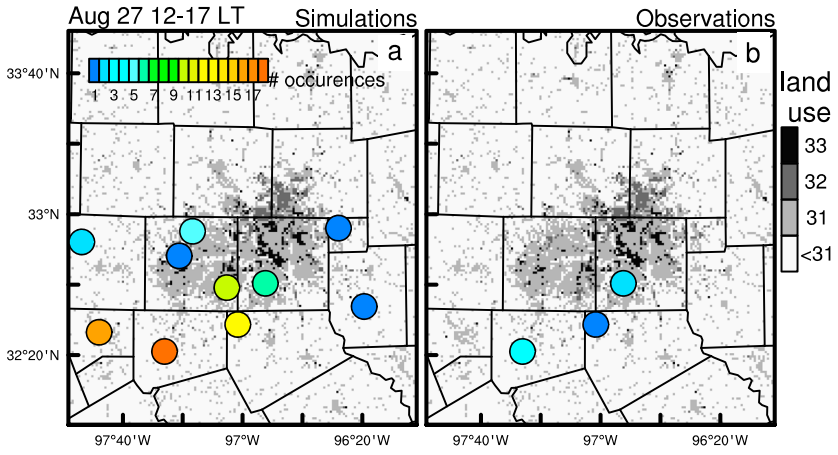

Figure 18. (a) Simulated and (b) observed locations and number of occurrences of maximum O_3 concentration in the DFW metropolitan area at each hour in the afternoon (i.e., 1200–1700 local time) of 27 August 2011.

O_3 diurnal cycle, while it has a lower capability to capture the decreasing stage in the O_3 diurnal cycle (i.e., the model predicts an overly quick decrease), as also seen in the time series in Figure 16.

Maximum hourly O_3 concentrations at the air quality sites in the DFW metropolitan area also indicate that the ensemble captures the direction of the O_3 plume in the afternoon of 27 August. The observed and simulated locations with the maximum hourly O_3 concentration at the 20 air quality sites around DFW at each hour from 1200 to 1700 CST are shown in Figure 18. These locations roughly indicate the direction of O_3 plumes. The observations indicate that the O_3 plumes from DFW extend to southwest during the afternoon of 27 August (Figure 18b). While certain individual members predict the O_3 plume to extend to the east and west of DFW, most members predict a similar plume direction as in the observations (Figure 18a). These results indicate that ensemble mean likely provides a better prediction for the direction of the pollutant plume than a randomly picked individual member. Improved prediction regarding the spatial distribution of pollutants can provide air quality information at a subcity scale for use in public health analyses and design of pollution mitigation strategies (Hudak, 2014).

4. Discussions of the Different Impacts of Synoptic Fronts on Surface O_3

Impacts of synoptic fronts on ambient air quality have been investigated in a few previous studies. Previously reported mechanisms/impacts are, however, not applicable to explain the severe O_3 pollution in DFW on 27 August 2011. Strong, fast-moving wintertime kata fronts were reported to be capable of transporting stratospheric O_3 down to the surface, increasing surface O_3 by ~6 ppbv (Kunz & Speth, 1997). Nighttime thunderstorm gust fronts were shown by Darby et al. (2002) to be able to transport residual layer O_3 to the surface and cause a sharp rise in surface O_3. Hu, Klein, Xue, Shapiro, et al. (2013) examined the impact of nocturnal cold front passages on near-surface O_3 concentration in Oklahoma. The vertical O_3 gradient is positive at night due to the titration reaction and dry deposition. During a nocturnal cold front passage, vertical mixing is enhanced due to enhanced vertical wind shear. Consequently, O_3-rich upper layer air is transported to the surface, leading to a nocturnal secondary O_3 maximum (Hu, Klein, Xue, Shapiro, et al., 2013). The impact of a change in the frequency of cold fronts associated with midlatitude baroclinic cyclones on U.S. air quality is investigated by Leibensperger et al. (2008). Cold fronts often push polluted continental air out over the Atlantic and replace it with cleaner air, thus improving air quality in United States. A recent decline in frequency of cold fronts may have offset some of the improvement of ambient air quality in United States (Leibensperger et al., 2008). None of those mechanisms/impacts, however, can explain the severe O_3 pollution during the daytime of 27 August 2011, ~40 ppbv higher than the more typical low-O_3 day.

For the case of 27 August 2011, the passage of the Hurricane Irene interrupted the Bermuda High in the Atlantic and helped a boundary layer high-pressure center over the Northern Plains to draw air southward over the eastern United States. Consequently, a front moved into Texas and persisted near DFW. The stagnant zone associated with the stationary front confined the urban plume from DFW and led to a high-O_3 episode. Coincidences between passages of the Atlantic Hurricanes and O_3 episodes in the DFW area (as well as other metropolitan areas nearby in the Southern Great Plains, e.g., the Oklahoma City) have also been found for other instances, including Hurricane Debby on 22–27 June 2012 and Hurricane Ernesto on 1 September 2006 (Hu, Zhang, et al., 2010; Nielsen-Gammon et al., 2010). Hurricane Ernesto is very similar to Hurricane Irene. Its landfall in North Carolina on 1 September 2006 brought a dead zone to the southwest of DFW (see Hu, Zhang, et al., 2010, Figure 2) and led to severe O_3 pollution. However, the impact of this Hurricane on the severe O_3 pollution in DFW was not previously realized or documented (Hu, Zhang, et al., 2010; Nielsen-Gammon et al., 2010; Parrish et al., 2009). As shown in the supporting information, WRF/Chem experiments are also conducted for this hurricane, which further confirms the role of Hurricane Ernesto in inducing a northwest-southeast oriented dead zone southwest of DFW, and the subsequent severe O_3 pollution over the DFW metropolitan area.

While the two cases (i.e., Irene and Ernesto) examined in this study demonstrated that Atlantic hurricanes can modify large-scale atmospheric circulations leading to flow stagnation and subsequent severe O_3 pollution over DFW, the presence of an Atlantic hurricane does not necessarily always induce flow stagnation in the area given the wide range of hurricane behaviors and paths (Evans et al., 2011). Many questions remain, such as the impacts of hurricanes with different sizes, strength, and paths, climatological correlation

between O_3 pollution and dead zones over DFW with the presence of hurricane. There may be many dead zone situations that are not related to an Atlantic hurricane. Full climatological studies are needed to answer some of the questions.

5. Conclusions

A severe O_3 pollution event on 27 August 2011 in the Dallas-Fort Worth (DFW) metropolitan area associated with the passage of Hurricane Irene along the eastern Atlantic coast is investigated in this study using observations from Meteorological Assimilation Data Ingest System, High Vertical Resolution Radiosonde Data, and TCEQ, and simulations with the WRF/Chem model. The passage of the Hurricane interrupted the Bermuda subtropic high in the Atlantic and helped a boundary layer high-pressure center over the Northern Plains to draw air southward over eastern United States. Consequently, a northwest-southeast oriented front moved into Texas and became stationary and persisted west of DFW. Winds transitioned from easterly/northeasterly to southwesterly across the front. In the transition zone, the flow was nearly stagnant. The stagnant zone blocked and confined the pollutant plume from DFW, leading to accumulation of primary pollutants and prominent boundary layer O_3 formation. Emission sources from a few urban areas east of DFW as well as power plants near Mount Pleasant and Carthage also partially contributed to this DFW O_3 pollution episode. Such a scenario on 27 August is in contrast to the typical summer days (e.g., 8 August 2011), on which southerly winds along the west edge of the Bermuda High prevail over the Southern Great Plains and the pollutant plumes from DFW are widely dispersed, leading to formation of light O_3 plumes. Different efficiency of midday O_3 production through chemical reactions during the two episodes is confirmed by process analyses. Sensitivity WRF/Chem simulations suppressing the hurricane confirms the role of Hurricane Irene breaking down the Bermuda High and inducing a dead zone and the subsequent severe O_3 pollution in the DFW metropolitan area. These analyses suggest that meteorological conditions, particularly wind transport, play an important role in modulating the characteristics (e.g., concentration, direction) of O_3 plumes.

Given the importance of meteorological fields (particularly transport) on modulating O_3 plumes, forecast errors in meteorological fields should play a very important role in inducing uncertainties in O_3 prediction, which is important to consider in air quality evaluations and policy decision-making. Thus, a 12-member SREF-WRF/Chem ensemble air quality forecasting system is demonstrated (by driving the WRF/Chem model using the SREF ensemble initial and boundary conditions) and run to assess the impact of meteorological uncertainties (particularly wind transport uncertainties) on urban air quality forecasting. While the ensemble system performs well in capturing the daytime O_3, it underestimates nighttime O_3 presumably due to the deficiency in the coupling between meteorological and chemical components in the WRF/Chem model. In contrast to the well-captured statistical O_3 values (i.e., median, maximum, and minimum) in the DFW metropolitan area during the day, the SREF-WRF/Chem ensemble prediction system gives a large spread in predicted O_3 plume direction. The ensemble gives a more reliable depiction of plume direction than any single member, which is critical for public health analysis.

Acknowledgments
This work was sponsored by the National Key R&D Program of China (grant 2016YFC0201900) and partially supported by funding from NASA NNX17AG11G. The second author was supported by NSF grants AGS-0941491, AGS-1046171, AGS-1046081, and AGS-1261776. Jun Du of NOAA/NCEP provided the SREF data. Proofreading by Nate Snook is greatly appreciated. Computations were performed at the Texas Advanced Computing Center (TACC). Model data produced from this study have been archived at University of Oklahoma, http://www.caps.ou.edu/micronet/HurricaneImpactonO3.html. The ERA-Interim, EPA air quality, MADIS, HVRRD, and stage IV data sets were retrieved from https://rda.ucar.edu/datasets/ds627.0/, https://aqs.epa.gov/aqsweb/airdata/download_files.html, https://madis.ncep.noaa.gov/, http://www.sparc-climate.org/data-centre/data-access/us-radiosonde/, and http://data.eol.ucar.edu/codiac/dss/id=21.093, respectively. Three anonymous reviewers and the Editor provided helpful comments that improved the manuscript.

References

Angell, J. K., Pack, D. H., Machta, L., Dickson, C. R., & Hoecker, W. H. (1972). Three-dimensional air trajectories determined from Tetroon flights in the planetary boundary layer of the Los Angeles Basin. *Journal of Applied Meteorology*, *11*(3), 451–471. https://doi.org/10.1175/1520-0450(1972)011<0451:TDATDF>2.0.CO;2

Banta, R. M., Senff, C. J., Nielsen-Gammon, J., Darby, L. S., Ryerson, T. B., Alvarez, R. J., et al. (2005). A bad air day in Houston. *Bulletin of the American Meteorological Society*, *86*(5), 657–670. https://doi.org/10.1175/Bams-86-5-657

Bao, J. W., Michelson, S. A., McKeen, S. A., & Grell, G. A. (2005). Meteorological evaluation of a weather-chemistry forecasting model using observations from the TEXAS AQS 2000 field experiment. *Journal of Geophysical Research*, *110*, D21105. https://doi.org/10.1029/2004JD005024

Bei, N. F., Li, G. H., Meng, Z. Y., Weng, Y. H., Zavala, M., & Molina, L. T. (2014). Impacts of using an ensemble Kalman filter on air quality simulations along the California-Mexico border region during cal-Mex 2010 field campaign. *Science of the Total Environment*, *499*, 141–153. https://doi.org/10.1016/j.scitotenv.2014.07.121

Bei, N. F., Xiao, B., Meng, N., & Feng, T. (2016). Critical role of meteorological conditions in a persistent haze episode in the Guanzhong basin, China. *Science of the Total Environment*, *550*, 273–284. https://doi.org/10.1016/j.scitotenv.2015.12.159

Black, T. L. (1994). The new Nmc mesoscale eta-model—Description and forecast examples. *Weather and Forecasting*, *9*(2), 265–278. https://doi.org/10.1175/1520-0434(1994)009<0265:Tnnmem>2.0.Co;2

Chatani, S., & Sharma, S. (2018). Uncertainties caused by major meteorological analysis data sets in simulating air quality over India. *Journal of Geophysical Research: Atmospheres*, *123*, 6230–6247. https://doi.org/10.1029/2017JD027502

Chen, F., & Dudhia, J. (2001). Coupling an advanced land surface-hydrology model with the Penn State-NCAR MM5 modeling system. Part I: Model implementation and sensitivity. *Monthly Weather Review*, *129*(4), 569–585. https://doi.org/10.1175/1520-0493(2001)129<0569:Caalsh>2.0.Co;2

Choi, Y., & Souri, A. H. (2015). Chemical condition and surface ozone in large cities of Texas during the last decade: Observational evidence from OMI, CAMS, and model analysis. *Remote Sensing of Environment*, *168*, 90–101. https://doi.org/10.1016/j.rse.2015.06.026

Cox, W. M., & Chu, S. H. (1996). Assessment of interannual ozone variation in urban areas from a climatological perspective. *Atmospheric Environment*, *30*(14), 2615–2625. https://doi.org/10.1016/1352-2310(95)00346-0

Darby, L. S. (2005). Cluster analysis of surface winds in Houston, Texas, and the impact of wind patterns on ozone. *Journal of Applied Meteorology*, *44*(12), 1788–1806. https://doi.org/10.1175/Jam2320.1

Darby, L. S., Banta, R. M., Brewer, W. A., Neff, W. D., Marchbanks, R. D., McCarty, B. J., et al. (2002). Vertical variations in O_3 concentrations before and after a gust front passage. *Journal of Geophysical Research*, *107*(D13), 4176. https://doi.org/10.1029/2001JD000996

Daum, P. H., Kleinman, L. I., Springston, S. R., Nunnermacker, L. J., Lee, Y. N., Weinstein-Lloyd, J., et al. (2003). A comparative study of O-3 formation in the Houston urban and industrial plumes during the 2000 Texas Air Quality Study. *Journal of Geophysical Research*, *108*(D23), 4715. https://doi.org/10.1029/2003JD003552

Daum, P. H., Kleinman, L. I., Springston, S. R., Nunnermacker, L. J., Lee, Y. N., Weinstein-Lloyd, J., et al. (2004). Origin and properties of plumes of high ozone observed during the Texas 2000 Air Quality Study (TexAQS 2000). *Journal of Geophysical Research*, *109*, D17306. https://doi.org/10.1029/2003JD004311

Delle Monache, L., Hacker, J. P., Zhou, Y. M., Deng, X. X., & Stull, R. B. (2006). Probabilistic aspects of meteorological and ozone regional ensemble forecasts. *Journal of Geophysical Research*, *111*, D24307. https://doi.org/10.1029/2005JD003917

Delle Monache, L., & Stull, R. B. (2003). An ensemble air-quality forecast over western Europe during an ozone episode. *Atmospheric Environment*, *37*(25), 3469–3474. https://doi.org/10.1016/S1352-2310(03)00475-8

Digar, A., Cohan, D. S., Xiao, X., Foley, K. M., Koo, B., & Yarwood, G. (2013). Constraining ozone-precursor responsiveness using ambient measurements. *Journal of Geophysical Research: Atmospheres*, *118*, 1005–1019. https://doi.org/10.1029/2012JD018100

Djalalova, I., Wilczak, J., McKeen, S., Grell, G., Peckham, S., Pagowski, M., et al. (2010). Ensemble and bias-correction techniques for air quality model forecasts of surface O-3 and $PM_{2.5}$ during the TEXAQS-II experiment of 2006. *Atmospheric Environment*, *44*(4), 455–467. https://doi.org/10.1016/j.atmosenv.2009.11.007

Du, J., Dimego, G., Toth, Z., Jovic, D., Zhou, B., Zhu, J., et al. (2009). Recent upgrade of NCEP short-range ensemble forecast (SREF) system. Paper presented at the 19th conf. On numerical weather prediction and 23rd conf. On weather analysis and forecasting, Omaha, NE.

Du, J., & Tracton, M. S. (2001). Implementation of a real-time short-range ensemble forecasting system at NCEP: An update. Paper presented at the 9th Conference on Mesoscale Processes, Ft. Lauderdale, Florida.

Dudhia, J. (1989). Numerical study of convection observed during the winter monsoon experiment using a mesoscale two-dimensional model. *Journal of the Atmospheric Sciences*, *46*(20), 3077–3107. https://doi.org/10.1175/1520-0469(1989)046<3077:Nsocod>2.0.Co;2

Emmons, L. K., Walters, S., Hess, P. G., Lamarque, J. F., Pfister, G. G., Fillmore, D., et al. (2010). Description and evaluation of the model for ozone and related chemical tracers, version 4 (MOZART-4). *Geoscientific Model Development*, *3*(1), 43–67. https://doi.org/10.5194/gmd-3-43-2010

Evans, J. L., Fuentes, J. D., Hu, X.-M., & Hamilton, H. (2011). Earth-atmosphere interactions: Tropical storm and hurricane activity in the Caribbean and their consequent health impacts. *Journal of Race and Policy*, *7*(1), 53–74. http://www.micromet.psu.edu/datatransfer/JenniPaper/files/Earth-Atmosphere_Interactions_FINAL.pdf

Fitzpatrick, P. J. (1997). Understanding and forecasting tropical cyclone intensity change with the typhoon intensity prediction scheme (TIPS). *Weather and Forecasting*, *12*(4), 826–846. https://doi.org/10.1175/1520-0434(1997)012<0826:Uaftci>2.0.Co;2

Galmarini, S., Kioutsioukis, I., & Solazzo, E. (2013). E pluribus unum*: Ensemble air quality predictions. *Atmospheric Chemistry and Physics*, *13*(14), 7153–7182. https://doi.org/10.5194/acp-13-7153-2013

Gilliam, R. C., Godowitch, J. M., & Rao, S. T. (2012). Improving the horizontal transport in the lower troposphere with four dimensional data assimilation. *Atmospheric Environment*, *53*, 186–201. https://doi.org/10.1016/j.atmosenv.2011.10.064

Gilliam, R. C., Hogrefe, C., Godowitch, J. M., Napelenok, S., Mathur, R., & Rao, S. T. (2015). Impact of inherent meteorology uncertainty on air quality model predictions. *Journal of Geophysical Research: Atmospheres*, *120*, 12,259–12,280. https://doi.org/10.1002/2015JD023674

Grell, G. A., Peckham, S. E., Schmitz, R., McKeen, S. A., Frost, G., Skamarock, W. C., & Eder, B. (2005). Fully coupled "online" chemistry within the WRF model. *Atmospheric Environment*, *39*(37), 6957–6975. https://doi.org/10.1016/j.atmosenv.2005.04.027

Guenther, A., Karl, T., Harley, P., Wiedinmyer, C., Palmer, P. I., & Geron, C. (2006). Estimates of global terrestrial isoprene emissions using MEGAN (model of emissions of gases and aerosols from nature). *Atmospheric Chemistry and Physics*, *6*, 3181–3210.

Han, Z. W., Ueda, H., & An, J. L. (2008). Evaluation and intercomparison of meteorological predictions by five MM5-PBL parameterizations in combination with three land-surface models. *Atmospheric Environment*, *42*(2), 233–249. https://doi.org/10.1016/j.atmosenv.2007.09.053

Homer, C., Dewitz, J., Yang, L. M., Jin, S., Danielson, P., Xian, G., et al. (2015). Completion of the 2011 National Land Cover Database for the conterminous United States—Representing a decade of land cover change information. *Photogrammetric Engineering and Remote Sensing*, *81*(5), 345–354. https://doi.org/10.14358/Pers.81.5.345

Hong, S. Y., Dudhia, J., & Chen, S. H. (2004). A revised approach to ice microphysical processes for the bulk parameterization of clouds and precipitation. *Monthly Weather Review*, *132*(1), 103–120. https://doi.org/10.1175/1520-0493(2004)132<0103:Aratim>2.0.Co;2

Hong, S. Y., Noh, Y., & Dudhia, J. (2006). A new vertical diffusion package with an explicit treatment of entrainment processes. *Monthly Weather Review*, *134*(9), 2318–2341. https://doi.org/10.1175/Mwr3199.1

Houze, R. A., & Betts, A. K. (1981). Convection in gate. *Reviews of Geophysics*, *19*(4), 541–576. https://doi.org/10.1029/RG019i004p00541

Hu, X.-M. (2008). *Incorporation of the Model of Aerosol Dynamics, Reaction, Ionization, and Dissolution (MADRID) into the Weather Research and Forecasting Model with Chemistry (WRF/Chem): Model Development and Retrospective Applications*. (PhD thesis), NC State University. Retrieved from http://repository.lib.ncsu.edu/ir/handle/1840.16/5241

Hu, X.-M., Doughty, D. C., Sanchez, K. J., Joseph, E., & Fuentes, J. D. (2012). Ozone variability in the atmospheric boundary layer in Maryland and its implications for vertical transport model. *Atmospheric Environment*, *46*, 354–364. https://doi.org/10.1016/j.atmosenv.2011.09.054

Hu, X.-M., Fuentes, J. D., & Zhang, F. (2010). Downward transport and modification of tropospheric ozone through moist convection. *Journal of Atmospheric Chemistry*, *65*(1), 13–35. https://doi.org/10.1007/s10874-010-9179-5

Hu, X.-M., Klein, P. M., & Xue, M. (2013). Evaluation of the updated YSU planetary boundary layer scheme within WRF for wind resource and air quality assessments. *Journal of Geophysical Research: Atmospheres*, *118*, 10,490–10,505. https://doi.org/10.1002/jgrd.50823

Hu, X.-M., Klein, P. M., Xue, M., Shapiro, A., & Nallapareddy, A. (2013). Enhanced vertical mixing associated with a nocturnal cold front passage and its impact on near-surface temperature and ozone concentration. *Journal of Geophysical Research: Atmospheres*, *118*, 2714–2728. https://doi.org/10.1002/jgrd.50309

Hu, X.-M., Nielsen-Gammon, J. W., & Zhang, F. Q. (2010). Evaluation of three planetary boundary layer schemes in the WRF model. *Journal of Applied Meteorology and Climatology*, *49*(9), 1831–1844. https://doi.org/10.1175/2010jamc2432.1

Hu, X.-M., & Xue, M. (2016). Influence of synoptic sea-breeze fronts on the urban heat island intensity in Dallas-Fort Worth, Texas. *Monthly Weather Review*, *144*(4), 1487–1507. https://doi.org/10.1175/Mwr-D-15-0201.1

Hu, X.-M., Xue, M., & McPherson, R. A. (2017). The importance of soil type contrast in modulating August precipitation distribution near the Edwards Plateau and Balcones escarpment in Texas. *Journal of Geophysical Research: Atmospheres*, *122*, 10,711–10,728. https://doi.org/10.1002/2017JD027035

Hu, X.-M., Zhang, F. Q., & Nielsen-Gammon, J. W. (2010). Ensemble-based simultaneous state and parameter estimation for treatment of mesoscale model error: A real-data study. *Geophysical Research Letters*, *37*, L08802. https://doi.org/10.1029/2010GL043017

Huang, J. P., Fung, J. C. H., Lau, A. K. H., & Qin, Y. (2005). Numerical simulation and process analysis of typhoon-related ozone episodes in Hong Kong. *Journal of Geophysical Research*, *110*, D05301. https://doi.org/10.1029/2004JD004914

Hudak, P. F. (2014). Spatial pattern of ground-level ozone concentration in Dallas-Fort Worth metropolitan area. *International Journal of Environmental Research*, *8*(4), 897–902.

Janjić, Z. I. (1990). The step-mountain coordinate: Physical package. *Monthly Weather Review*, *118*(7), 1429–1443. https://doi.org/10.1175/1520-0493(1990)118<1429:TSMCPP>2.0.CO;2

Jiang, G. F., & Fast, J. D. (2004). Modeling the effects of VOC and NO_x emission sources on ozone formation in Houston during the TexAQS 2000 field campaign. *Atmospheric Environment*, *38*(30), 5071–5085. https://doi.org/10.1016/j.atmosenv.2004.06.012

Jiang, Y. C., Zhao, T. L., Liu, J., Xu, X. D., Tan, C. H., Cheng, X. H., et al. (2015). Why does surface ozone peak before a typhoon landing in Southeast China? *Atmospheric Chemistry and Physics*, *15*(23), 13,331–13,338. https://doi.org/10.5194/acp-15-13331-2015

Juang, H. M. H., & Kanamitsu, M. (1994). The Nmc nested regional spectral model. *Monthly Weather Review*, *122*(1), 3–26. https://doi.org/10.1175/1520-0493(1994)122<0003:Tnnrsm>2.0.Co;2

Juneng, L., Tangang, F. T., & Reason, C. J. C. (2007). Numerical case study of an extreme rainfall event during 9–11 December 2004 over the east coast of peninsular Malaysia. *Meteorology and Atmospheric Physics*, *98*(1-2), 81–98. https://doi.org/10.1007/s00703-006-0236-1

Karl, T., Jobson, T., Kuster, W. C., Williams, E., Stutz, J., Shetter, R., et al. (2003). Use of proton-transfer-reaction mass spectrometry to characterize volatile organic compound sources at the La Porte super site during the Texas Air Quality Study 2000. *Journal of Geophysical Research*, *108*(D16), 4508. https://doi.org/10.1029/2002JD003333

Kemball-Cook, S., Parrish, D., Ryerson, T., Nopmongcol, U., Johnson, J., Tai, E., & Yarwood, G. (2009). Contributions of regional transport and local sources to ozone exceedances in Houston and Dallas: Comparison of results from a photochemical grid model to aircraft and surface measurements. *Journal of Geophysical Research*, *114*, D00f02. https://doi.org/10.1029/2008JD010248

Kim, S., Byun, D. W., & Cohan, D. (2009). Contributions of inter- and intra-state emissions to ozone over Dallas-Fort Worth, Texas. *Civil Engineering and Environmental Systems*, *26*(1), 103–116. https://doi.org/10.1080/10286600802005364

Kim, S. W., McKeen, S. A., Frost, G. J., Lee, S. H., Trainer, M., Richter, A., et al. (2011). Evaluations of NO_x and highly reactive VOC emission inventories in Texas and their implications for ozone plume simulations during the Texas air quality study 2006. *Atmospheric Chemistry and Physics*, *11*(22), 11,361–11,386. https://doi.org/10.5194/acp-11-11361-2011

Kim, Y., Fu, J. S., & Miller, T. L. (2010). Improving ozone modeling in complex terrain at a fine grid resolution: Part I—examination of analysis nudging and all PBL schemes associated with LSMs in meteorological model. *Atmospheric Environment*, *44*(4), 523–532. https://doi.org/10.1016/j.atmosenv.2009.10.045

Klein, P. M., Hu, X.-M., Shapiro, A., & Xue, M. (2015). Linkages between boundary-layer structure and the development of nocturnal low-level jets in central Oklahoma. *Boundary-Layer Meteorology*, 1–26. https://doi.org/10.1007/s10546-015-0097-6

Klein, P. M., Hu, X.-M., & Xue, M. (2014). Impacts of mixing processes in nocturnal atmospheric boundary layer on urban ozone concentrations. *Boundary-Layer Meteorology*, *150*(1), 107–130. https://doi.org/10.1007/s10546-013-9864-4

Kleinman, L. I., Daum, P. H., Imre, D., Lee, Y. N., Nunnermacker, L. J., Springston, S. R., et al. (2002). Ozone production rate and hydrocarbon reactivity in 5 urban areas: A cause of high ozone concentration in Houston. *Geophysical Research Letters*, *29*(10), 1467. https://doi.org/10.1029/2001GL014569

Kleinman, L. I., Daum, P. H., Lee, Y. N., Nunnermacker, L. J., Springston, S. R., Weinstein-Lloyd, J., & Rudolph, J. (2005). A comparative study of ozone production in five U.S. metropolitan areas. *Journal of Geophysical Research*, *110*, D02301. https://doi.org/10.1029/2004JD005096

Kulkarni, P. S., Bortoli, D., Silva, A. M., & Reeves, C. E. (2015). Enhancements in nocturnal surface ozone at urban sites in the UK. *Environmental Science and Pollution Research*, *22*(24), 20,295–20,305.

Kunz, H., & Speth, P. (1997). Variability of near-ground ozone concentrations during cold front passages—A possible effect of tropopause folding events. *Journal of Atmospheric Chemistry*, *28*(1–3), 77–95. https://doi.org/10.1023/A:1005867229466

Kusaka, H., Kondo, H., Kikegawa, Y., & Kimura, F. (2001). A simple single-layer urban canopy model for atmospheric models: Comparison with multi-layer and slab models. *Boundary-Layer Meteorology*, *101*(3), 329–358. https://doi.org/10.1023/A:1019207923078

Langford, A. O., Senff, C. J., Alvarez, R. J., Banta, R. M., Hardesty, R. M., Parrish, D. D., & Ryerson, T. B. (2011). Comparison between the TOPAZ airborne ozone lidar and in situ measurements during TexAQS 2006. *Journal of Atmospheric and Oceanic Technology*, *28*(10), 1243–1257. https://doi.org/10.1175/Jtech-D-10-05043.1

Lei, R. X., Talbot, R., Wang, Y. X., Wang, S. C., & Estes, M. (2018). Influence of cold fronts on variability of daily surface O-3 over the Houston-Galveston-Brazoria area in Texas USA during 2003–2016. *Atmosphere*, *9*(5), 159. https://doi.org/10.3390/atmos9050159

Leibensperger, E. M., Mickley, L. J., & Jacob, D. J. (2008). Sensitivity of US air quality to mid-latitude cyclone frequency and implications of 1980–2006 climate change. *Atmospheric Chemistry and Physics*, *8*(23), 7075–7086.

Ludwig, F. L., & Shelar, E. (1978). Effects of weather fronts on ozone transport. In A. L. Morris & R. C. Barras (Eds.), *Air Quality Meteorology and Atmospheric Ozone* (pp. 389–406). West Conshohocken, PA: American Society for Testing and Materials. https://doi.org/10.1520/STP36597S

Luria, M., Valente, R. J., Bairai, S., Parkhurst, W. J., & Tanner, R. L. (2008). Airborne study of ozone formation over Dallas, Texas. *Atmospheric Environment*, *42*(29), 6951–6958. https://doi.org/10.1016/j.atmosenv.2008.04.057

Lyons, W. A., Tremback, C. J., & Pielke, R. A. (1995). Applications of the regional atmospheric modeling system (RAMS) to provide input to photochemical grid models for the Lake-Michigan ozone study (LMOS). *Journal of Applied Meteorology*, *34*(8), 1762–1786. https://doi.org/10.1175/1520-0450(1995)034<1762:Aotram>2.0.Co;2

Marecal, V., Peuch, V. H., Andersson, C., Andersson, S., Arteta, J., Beekmann, M., et al. (2015). A regional air quality forecasting system over Europe: The MACC-II daily ensemble production. *Geoscientific Model Development*, *8*(9), 2777–2813. https://doi.org/10.5194/gmd-8-2777-2015

Martins, D. K., Stauffer, R. M., Thompson, A. M., Knepp, T. N., & Pippin, M. (2012). Surface ozone at a coastal suburban site in 2009 and 2010: Relationships to chemical and meteorological processes. *Journal of Geophysical Research*, *117*, D05306. https://doi.org/10.1029/2011JD016828

Matichuk, R., Tonnesen, G., Luecken, D., Gilliam, R., Napelenok, S. L., Baker, K. R., et al. (2017). Evaluation of the community multiscale air quality model for simulating winter ozone formation in the Uinta Basin. *Journal of Geophysical Research: Atmospheres*, *122*, 13,545–13,572. https://doi.org/10.1002/2017JD027057

McKeen, S., Grell, G., Peckham, S., Wilczak, J., Djalalova, I., Hsie, E. Y., et al. (2009). An evaluation of real-time air quality forecasts and their urban emissions over eastern Texas during the summer of 2006 Second Texas Air Quality Study field study. *Journal of Geophysical Research*, *114*, D00f11. https://doi.org/10.1029/2008JD011697

McKeen, S., Wilczak, J., Grell, G., Djalalova, I., Peckham, S., Hsie, E. Y., et al. (2005). Assessment of an ensemble of seven real-time ozone forecasts over eastern North America during the summer of 2004. *Journal of Geophysical Research*, *110*, D21307. https://doi.org/10.1029/2005JD005858

McNider, R. T., Doty, K., Norris, W. B., & Biazar, A. (2005). Conceptual model for extreme ozone concentration events in Dallas and East Texas based on reduced dilution in frontal zones. Texas.

Miao, Y., Hu, X.-M., Liu, S., Qian, T., Xue, M., Zheng, Y., & Wang, S. (2015). Seasonal variation of local atmospheric circulations and boundary layer structure in the Beijing-Tianjin-Hebei region and implications for air quality. *Journal of Advances in Modeling Earth Systems*, *7*, 1602–1626. https://doi.org/10.1002/2015MS000522

Mlawer, E. J., Taubman, S. J., Brown, P. D., Iacono, M. J., & Clough, S. A. (1997). Radiative transfer for inhomogeneous atmospheres: RRTM, a validated correlated-*k* model for the longwave. *Journal of Geophysical Research*, *102*(D14), 16,663–16,682. https://doi.org/10.1029/97JD00237

Monteiro, A., Ribeiro, I., Tchepel, O., Carvalho, A., Martins, H., Sá, E., et al. (2013). Ensemble techniques to improve air quality assessment: Focus on O-3 and PM. *Environmental Modeling and Assessment*, *18*(3), 249–257. https://doi.org/10.1007/s10666-012-9344-0

Nielsen-Gammon, J. W., Hu, X.-M., Zhang, F., & Pleim, J. E. (2010). Evaluation of planetary boundary layer scheme sensitivities for the purpose of parameter estimation. *Monthly Weather Review*, *138*(9), 3400–3417. https://doi.org/10.1175/2010mwr3292.1

Palmer, T., Molteni, F., Mureau, R., Buizza, R., Chapelet, P., & Tribbia, J. (1992). Ensemble prediction (188). Retrieved from Shinfield Park, Reading: https://www.ecmwf.int/en/elibrary/11560-ensemble-prediction

Parrish, D. D., Allen, D. T., Bates, T. S., Estes, M., Fehsenfeld, F. C., Feingold, G., et al. (2009). Overview of the Second Texas Air Quality Study (TexAQS II) and the Gulf of Mexico Atmospheric Composition and Climate Study (GoMACCS). *Journal of Geophysical Research*, *114*, D00f13. https://doi.org/10.1029/2009JD011842

Pielke, R. A. (1998). The need to assess uncertainty in air quality evaluations. *Atmospheric Environment*, *32*(8), 1467–1468. https://doi.org/10.1016/S1352-2310(97)00435-4

Pierce, R. B., al-Saadi, J., Kittaka, C., Schaack, T., Lenzen, A., Bowman, K., Szykman, J., et al. (2009). Impacts of background ozone production on Houston and Dallas, Texas, air quality during the Second Texas Air Quality Study field mission. *Journal of Geophysical Research*, *114*, D00f09. https://doi.org/10.1029/2008JD011337

Pleim, J., Gilliam, R., Appel, W., & Ran, L. (2016). Recent advances in modeling of the atmospheric boundary layer and land surface in the coupled WRF-CMAQ model. In D. G. Steyn & N. Chaumerliac (Eds.), *Air Pollution Modeling and its Application XXIV*. Cham: Springer International Publishing. https://doi.org/10.1007/978-3-319-24478-5_64

Pleim, J. E. (2011). Comment on "Simulation of surface ozone pollution in the central Gulf Coast region using WRF/Chem model: Sensitivity to PBL and land surface physics". *Advances in Meteorology*, *2011*, 464753. https://doi.org/10.1155/2011/464753

Pongprueksa, P. (2013). Application of satellite data in a regional model to improve long-term ozone simulations. *Journal of Atmospheric Chemistry*, *70*(4), 317–340. https://doi.org/10.1007/s10874-013-9270-9

Qin, Y., Walk, T., Gary, R., Yao, X., & Elles, S. (2007). C-2–C-10 nonmethane hydrocarbons measured in Dallas, USA—Seasonal trends and diurnal characteristics. *Atmospheric Environment*, *41*(28), 6018–6032. https://doi.org/10.1016/j.atmosenv.2007.03.008

Rappengluck, B., Perna, R., Zhong, S. Y., & Morris, G. A. (2008). An analysis of the vertical structure of the atmosphere and the upper-level meteorology and their impact on surface ozone levels in Houston, Texas. *Journal of Geophysical Research*, *113*, D17315. https://doi.org/10.1029/2007JD009745

Ryerson, T. B., Trainer, M., Angevine, W. M., Brock, C. A., Dissly, R. W., Fehsenfeld, F. C., et al. (2003). Effect of petrochemical industrial emissions of reactive alkenes and NO_x on tropospheric ozone formation in Houston, Texas. *Journal of Geophysical Research*, *108*(D8), 4249. https://doi.org/10.1029/2002JD003070

Sandu, A., Daescu, D. N., & Carmichael, G. R. (2003). Direct and adjoint sensitivity analysis of chemical kinetic systems with KPP: Part I—Theory and software tools. *Atmospheric Environment*, *37*(36), 5083–5096. https://doi.org/10.1016/j.atmosenv.2003.08.019

Sather, M. E., & Cavender, K. (2012). Update of long-term trends analysis of ambient 8-hour ozone and precursor monitoring data in the south central U.S.; encouraging news. *Journal of Environmental Monitoring*, *14*(2), 666–676. https://doi.org/10.1039/c2em10862c

Seigneur, C., Pun, B., Pai, P., Louis, J. F., Solomon, P., Emery, C., Morris, R., et al. (2000). Guidance for the performance evaluation of three-dimensional air quality modeling systems for particulate matter and visibility. *Journal of the Air & Waste Management Association*, *50*(4), 588–599. https://doi.org/10.1080/10473289.2000.10464036

Senff, C. J., Alvarez, R. J., Hardesty, R. M., Banta, R. M., & Langford, A. O. (2010). Airborne lidar measurements of ozone flux downwind of Houston and Dallas. *Journal of Geophysical Research*, *115*, D20307. https://doi.org/10.1029/2009JD013689

Sillman, S. (1999). The relation between ozone, NO_x and hydrocarbons in urban and polluted rural environments. *Atmospheric Environment*, *33*(12), 1821–1845. https://doi.org/10.1016/S1352-2310(98)00345-8

Skamarock, W. C., J. B. Klemp, J. Dudhia, D. O. Gill, D. M. Barker, M. G. Duda, X.-Y. Huang, et al. (2008). A description of the Advanced Research WRF version 3. Boulder, CO.

Stauffer, R., & Thompson, A. (2015). Bay breeze climatology at two sites along the Chesapeake Bay from 1986–2010: Implications for surface ozone. *Journal of Atmospheric Chemistry*, *72*(3-4), 355–372. https://doi.org/10.1007/s10874-013-9260-y

Stauffer, R. M., Thompson, A. M., Martins, D. K., Clark, R. D., Goldberg, D. L., Loughner, C. P., Delgado, R., et al. (2015). Bay breeze influence on surface ozone at Edgewood, MD during July 2011. *Journal of Atmospheric Chemistry*, *72*(3-4), 335–353. https://doi.org/10.1007/s10874-012-9241-6

Stensrud, D. J., Brooks, H. E., Du, J., Tracton, M. S., & Rogers, E. (1999). Using ensembles for short-range forecasting. *Monthly Weather Review*, *127*(4), 433–446. https://doi.org/10.1175/1520-0493(1999)127<0433:Uefsrf>2.0.Co;2

Stockwell, W. R., Kirchner, F., Kuhn, M., & Seefeld, S. (1997). A new mechanism for regional atmospheric chemistry modeling. *Journal of Geophysical Research*, *102*(D22), 25,847–25,879. https://doi.org/10.1029/97JD00849

Taraphdar, S., Mukhopadhyay, P., Leung, L. R., Zhang, F. Q., Abhilash, S., & Goswami, B. N. (2014). The role of moist processes in the intrinsic predictability of Indian Ocean cyclones. *Journal of Geophysical Research: Atmospheres*, *119*, 8032–8048. https://doi.org/10.1002/2013JD021265

Tory, K. J., & Dare, R. A. (2015). Sea surface temperature thresholds for tropical cyclone formation. *Journal of Climate*, *28*(20), 8171–8183. https://doi.org/10.1175/Jcli-D-14-00637.1

Toth, Z., & Kalnay, E. (1997). Ensemble forecasting at NCEP and the breeding method. *Monthly Weather Review*, *125*(12), 3297–3319. https://doi.org/10.1175/1520-0493(1997)125<3297:Efanat>2.0.Co;2

Tracton, M. S., Du, J., Toth, Z., & Juang, H. (1998). Short-range ensemble forecasting (SREF) at NCEP/EMC. Paper presented at the 12th conf. On numerical weather prediction, Phoenix.

Vautard, R., Schaap, M., Bergström, R., Bessagnet, B., Brandt, J., Builtjes, P. J. H., et al. (2009). Skill and uncertainty of a regional air quality model ensemble. *Atmospheric Environment*, *43*(31), 4822–4832. https://doi.org/10.1016/j.atmosenv.2008.09.083

Wang, T., & Kwok, J. Y. H. (2003). Measurement and analysis of a multiday photochemical smog episode in the Pearl River delta of China. *Journal of Applied Meteorology*, *42*(3), 404–416. https://doi.org/10.1175/1520-0450(2003)042<0404:Maaoam>2.0.Co;2

Wei, X., Lam, K.-S., Cao, C., Li, H., & He, J. (2016). Dynamics of the typhoon Haitang related high ozone episode over Hong Kong. *Advances in Meteorology*, *2016*, 12. https://doi.org/10.1155/2016/6089154

Wert, B. P., Trainer, M., Fried, A., Ryerson, T. B., Henry, B., Potter, W., et al. (2003). Signatures of terminal alkene oxidation in airborne formaldehyde measurements during TexAQS 2000. *Journal of Geophysical Research*, *108*(D3), 4104. https://doi.org/10.1029/2002JD002502

Wilczak, J. M., Djalalova, I., McKeen, S., Bianco, L., Bao, J. W., Grell, G., et al. (2009). Analysis of regional meteorology and surface ozone during the TexAQS II field program and an evaluation of the NMM-CMAQ and WRF-Chem air quality models. *Journal of Geophysical Research*, *114*, D00f14. https://doi.org/10.1029/2008JD011675

Yamamoto, M. (2012). Rapid merger and recyclogenesis of twin extratropical cyclones leading to heavy precipitation around Japan on 9–10 October 2001. *Meteorological Applications*, *19*(1), 36–53. https://doi.org/10.1002/met.255

Yang, J. X., Lau, A. K. H., Fung, J. C. H., Zhou, W., & Wenig, M. (2012). An air pollution episode and its formation mechanism during the tropical cyclone Nuri's landfall in a coastal city of South China. *Atmospheric Environment*, *54*, 746–753. https://doi.org/10.1016/j.atmosenv.2011.12.023

Yu, S. C., Eder, B., Dennis, R., Chu, S. H., & Schwartz, S. E. (2006). New unbiased symmetric metrics for evaluation of air quality models. *Atmospheric Science Letters*, *7*(1), 26–34. https://doi.org/10.1002/asl.125

Yu, S., Mathur, R., Pleim, J., Pouliot, G., Wong, D., Eder, B., et al. (2012). Comparative evaluation of the impact of WRF-NMM and WRF-ARW meteorology on CMAQ simulations for O-3 and related species during the 2006 TexAQS/GoMACCS campaign. *Atmospheric Pollution Research*, *3*(2), 149–162. https://doi.org/10.5094/Apr.2012.015

Zhang, F. Q., Bei, N. F., Nielsen-Gammon, J. W., Li, G. H., Zhang, R. Y., Stuart, A., & Aksoy, A. (2007). Impacts of meteorological uncertainties on ozone pollution predictability estimated through meteorological and photochemical ensemble forecasts. *Journal of Geophysical Research*, *112*, D04304. https://doi.org/10.1029/2006JD007429

Zhang, F. Q., Koch, S. E., & Kaplan, M. L. (2003). Numerical simulations of a large-amplitude mesoscale gravity wave event. *Meteorology and Atmospheric Physics*, *84*(3-4), 199–216. https://doi.org/10.1007/s00703-002-0594-2

Zhang, H., Chen, G., Hu, J., Chen, S.-H., Wiedinmyer, C., Kleeman, M., & Ying, Q. (2014). Evaluation of a seven-year air quality simulation using the Weather Research and Forecasting (WRF)/Community Multiscale Air Quality (CMAQ) models in the eastern United States. *Science of the Total Environment*, *473–474*, 275–285. https://doi.org/10.1016/j.scitotenv.2013.11.121

Zhang, H., Li, J., Ying, Q., Guven, B. B., & Olaguer, E. P. (2013). Source apportionment of formaldehyde during TexAQS 2006 using a source-oriented chemical transport model. *Journal of Geophysical Research: Atmospheres*, *118*, 1525–1535. https://doi.org/10.1002/jgrd.50197

Zhang, H., & Ying, Q. (2011). Contributions of local and regional sources of NO_x to ozone concentrations in Southeast Texas. *Atmospheric Environment*, *45*(17), 2877–2887.

Zhu, J. H., & Liang, X. Z. (2013). Impacts of the Bermuda High on regional climate and ozone over the United States. *Journal of Climate*, *26*(3), 1018–1032. https://doi.org/10.1175/Jcli-D-12-00168.1